Hepatocyte-specific deletion of TIPARP, a negative regulator of the aryl hydrocarbon receptor, is sufficient to increase sensitivity to dioxin-induced wasting syndrome

David Hutin[1], Laura Tamblyn[1], Alvin Gomez[1], Giulia Grimaldi[2], Helen Soedling[2], Tiffany Cho[1], Shaimaa Ahmed[1], Christin Lucas[2], Chakravarthi Kanduri[3], Denis M. Grant[1] and Jason Matthews[1,2*]

[1]Department of Pharmacology and Toxicology, University of Toronto, Toronto, Canada. [2]Department of Nutrition, Institute of Basic Medical Sciences, University of Oslo, Oslo, Norway. [3]Jebsen Centre of Excellence for Celiac Disease Research, University of Oslo, Oslo, Norway.

Running Title: Hepatocyte-specific deletion of TIPARP increases dioxin toxicity

*To whom correspondence should be addressed: Jason Matthews, Department of Nutrition, Institute of Basic Medical Sciences, University of Oslo, Sognsvannsveien 9, 0372 Oslo; Email: jason.matthews@medisin.uio.no

Abstract

The aryl hydrocarbon receptor (AHR) mediates the toxic effects of dioxin (2,3,7,8-tetrachlorodibenzo-*p*-dioxin; TCDD), which include thymic atrophy, steatohepatitis, and a lethal wasting syndrome in laboratory rodents. Although the mechanisms of dioxin toxicity remain unknown, AHR signaling in hepatocytes is necessary for dioxin-induced liver toxicity. We previously reported that loss of TCDD-inducible poly(ADP-ribose) polymerase (TIPARP/PARP7/ARTD14), an AHR target gene and mono-ADP-ribosyltransferase, increases the sensitivity of mice to dioxin-induced toxicities. To test the hypothesis that TIPARP is a negative regulator of AHR signaling in hepatocytes, we generated *Tiparp*$^{fl/fl}$ mice in which exon 3 of *Tiparp* is flanked by loxP sites, followed by Cre-lox technology to create hepatocyte-specific (*Tiparp*$^{fl/fl}$*Cre*^{Alb}) and whole-body (*Tiparp*$^{fl/fl}$*Cre*^{CMV}*; Tiparp*$^{Ex3-/-}$) Tiparp null mice. *Tiparp*$^{fl/fl}$*Cre*^{Alb} and *Tiparp*$^{Ex3-/-}$ mice given a single injection of 10 μg/kg dioxin did not survive beyond day 7 and 9, respectively, while all *Tiparp*$^{+/+}$ mice survived the 30-day treatment. Dioxin-exposed *Tiparp*$^{fl/fl}$*Cre*^{Alb} and *Tiparp*$^{Ex3-/-}$ mice had increased steatohepatitis and hepatotoxicity as indicated by greater staining of neutral lipids and serum alanine aminotransferase activity than similarly treated wild-type mice. *Tiparp*$^{fl/fl}$*Cre*^{Alb} and *Tiparp*$^{Ex3-/-}$ mice exhibited augmented AHR signalling, denoted by increased dioxin-induced gene expression. Metabolomic studies revealed alterations in lipid and amino acid metabolism in liver extracts from *Tiparp*$^{fl/fl}$*Cre*^{Alb} mice compared with wild-type mice. Taken together, these data illustrate that TIPARP is an important negative regulator of AHR activity, and that its specific loss in hepatocytes is sufficient to increase sensitivity to dioxin-induced steatohepatitis and lethality.

Keywords: aryl hydrocarbon receptor, wasting syndrome, ADP-ribosylation, 2,3,7,8-tetrachlorodibenzo-p-dioxin, TCDD-inducible poly-ADP-ribose polymerase

Introduction

2,3,7,8-Tetrachlorodibenzo-*p*-dioxin (TCDD; dioxin) is a highly toxic environmental contaminant produced during waste incineration and other high-temperature industrial processes, and it remains a global health concern. The toxic effects of dioxin are mediated through its binding to and activation of the aryl hydrocarbon receptor (AHR), which is a member of the basic helix-loop-helix (bHLH) Period-AHR nuclear translocator (ARNT)-Single-minded (PAS) family of transcription factors. In the canonical AHR signaling pathway, ligand binding to cytosolic AHR causes its translocation to the nucleus where it dimerizes with ARNT (also known as hypoxia-inducible factor 1β; HIF1β). The AHR:ARNT heterodimer then binds DNA sequence elements (termed AHREs or DREs) located within the regulatory regions of its target genes, which include *cytochrome P4501A1* (*CYP1A1*), *CYP1B1* and TCDD-inducible ADP-ribose polymerase (TIPARP)(Ma *et al.*, 2001; Whitlock, 1999; Zhang *et al.*, 1998). In addition to its roles in dioxin toxicity, xenobiotic metabolism and vascular development (Stevens *et al.*, 2009), AHR has important roles in T-cell differentiation, in the defense against bacterial infections and in gut homeostasis (Moura-Alves *et al.*, 2014; Quintana *et al.*, 2008). To date, more than 400 AHR ligands have been identified, including dietary compounds (3,3'-diindolylmethane), various endogenous ligands (kynurenine, 6-formylindolo(3,2b)carbazole; FICZ), and environmental contaminants such as dioxin (Denison *et al.*, 2003).

Dioxin causes diverse toxic effects in laboratory rodents including immunosuppression, steatohepatitis, impaired reproduction and a lethal wasting syndrome (Birnbaum, 1994, 1995; Poland *et al.*, 1982). A single dose of dioxin induces a lethal starvation-like syndrome, which includes decreased gluconeogenesis, liver damage, steatohepatitis and dyslipidaemia, ultimately leading to lethality (Linden *et al.*, 2010; Seefeld *et al.*, 1984). Acute lethality varies widely both among species and between rodent strains. For example, the median lethal dose (LD_{50}) for guinea pigs is 1-2 μg/kg dioxin, whereas the LD_{50} for hamsters is >5000 μg/kg (Pohjanvirta *et al.*, 1994; Poland, et al., 1982). In most strains of mice, lethality occurs only 2-3 weeks after a single dose of 115-300 μg/kg of dioxin (Pohjanvirta, et al., 1994; Poland, et al., 1982). There is a roughly 10-fold difference in susceptibility between the high sensitivity C57BL/6 (Ahr^{b1} allele) and low sensitivity DBA/2 (Ahr^{d} allele) mouse strains, which is due to polymorphic variations in their ligand-binding domains (Poland *et al.*, 1994). The molecular mechanisms of dioxin-induced wasting syndrome remain obscure, but transgenic mice overexpressing AHR show increased sensitivity to dioxin toxicities, whereas $Ahr^{-/-}$ null and Ahr^{dbd} mice, which express a mutant AHR that does not bind to AHREs, are resistant to the effects of dioxin (Fernandez-Salguero *et al.*, 1996; Lee *et al.*, 2010; Walisser *et al.*, 2005).

TIPARP (PARP7/ARTD14) is an AHR-regulated gene and a member of the poly-adenosine diphosphate (ADP)-ribose) polymerase (PARP) family. PARPs are nicotinamide adenine dinucleotide (NAD^+)-dependent enzymes that use NAD^+ as a substrate to transfer one molecule of ADP-ribose, referred to as mono-ADP-ribosylation (MARylation), or several ADP-ribose moieties, referred to as poly-ADP-ribosylation (PARylation), to specific amino acid residues on themselves and on target proteins (Hottiger *et al.*, 2010). Mono- and poly-ADP-ribosylation are reversible post-translational modifications involved in several biological processes, such as immune cell function, regulation of transcription, protein expression and DNA repair (Kraus *et al.*, 2013). We previously reported that TIPARP is a mono-ADP-ribosyltransferase that functions as part of a negative feedback loop to repress AHR activity through a mechanism that involves reduced ligand-induced AHR protein levels and that requires TIPARP's catalytic activity (MacPherson *et al.*, 2013). Moreover, *Tiparp*$^{-/-}$ mice exhibit increased AHR activity but also increased sensitivity to dioxin-induced toxicities, including steatohepatitis, hepatotoxicity and lethal wasting syndrome (Ahmed *et al.*, 2015). Although the mechanisms of dioxin-induced toxicity remain incompletely understood, AHR expression in hepatocytes is needed to generate the adaptive as well as toxic response to dioxin exposure (Walisser, et al., 2005).

Here, we describe the generation of *Tiparp* conditional mutant mice in which exon 3 of the *Tiparp* gene is flanked by loxP sites, and the subsequent creation of both hepatocyte-specific (*Tiparp*$^{fl/fl}$*Cre*^{Alb}) and whole-body (*Tiparp*$^{fl/fl}$*Cre*^{CMV}*; Tiparp*$^{Ex3-/-}$) TIPARP knockout mice. These mice were used to further investigate the role of TIPARP in AHR signaling and dioxin-induced toxicity.

Materials and Methods

Generation of conditional Tiparp null mice - *Tiparp*$^{fl/fl}$ mice, where exon 3 of *Tiparp* was flanked by loxP sites, were generated from embryonic stem (ES) cells purchased from European Conditional Mouse Mutagenesis (EUCOMM; Tiparp$^{tm1a(EUCOMM)Wtsi}$). ES cells were expanded by the Toronto Centre for Phenogenomics (TCP). Correct targeted recombination was confirmed in 2 of 5 ES cell clones purchased. Briefly, SphI-digested genomic DNA was used in Southern blotting to produce 8.9 kb (wild-type) and 12.3 kb (tm1a) fragments spanning the 5` region of the targeted sequence of *Tiparp,* and in the targeted allele, including the neomycin-resistance (Neo) cassette. The Neo probe was used to reveal additional or random integrations of the targeting vector in the genomes (fragments of incorrect sizes); these ES clones were excluded. PCR primers used to generate the respective probes are provided in **Supplementary Table S1**. Based on the positive Southern blot results, ES cell clones D3 and G3 were chosen for aggregation and implantation into pseudopregnant surrogate females (performed by TCP). Chimeric *Tiparp*$^{+/tm1a}$ mice were bred to C57BL/6 albino females and pups were genotyped to identify those with germline transmission of the conditional mutant Tiparp allele (*Tiparp*$^{+/tm1a}$); only ES clone G3 resulted in successful germline transmission. Some *Tiparp*$^{+/tm1a}$ mice were bred to B6.C-Tg(CMV-cre)1Cgn/J (Jackson Labs, Bar Harbor, ME) to remove the Neo cassette and the targeted exon and leave the *lacZ* reporter gene (conversion to *tm1b* allele) and then outbred once to C57BL/6N to remove Tg-(CMV-cre). Mice heterozygous for the *tm1b* allele were then intercrossed to make homozygous *tm1b* mice (*Tiparp*$^{tm1b/tm1b}$, referred to as *Tiparp*$^{Ex3-/-}$). Other *Tiparp*$^{+/tm1a}$ mice were bred to B6(C3)-Tg(Pgk1-FLPo)10Sykr/J (Jackson Labs, Bar Harbor, ME) to remove the *lacZ* and *Neo* cassettes and leave the targeted exon flanked by LoxP sites (conversion to *tm1c* allele) and then outbred once to C57BL/6N to remove Tg-(Pgk1-FLPo) (*Tiparp*$^{+/tm1c}$). *Tiparp*$^{+/tm1c}$ mice were bred to B6.C-Tg(CMV-cre)1Cgn/J to remove the targeted exon (conversion to *tm1d* allele) and then outbred once to C57BL/6N to remove Tg-(CMV-cre). Mice heterozygous for the *tm1d* allele were then intercrossed to make homozygous *tm1d* mice (*Tiparp*$^{tm1d/tm1d}$; referred to as *Tiparp*$^{Ex3-/-}$). *Tiparp*$^{+/tm1c}$ mice were also bred to B6N.Cg-Tg(Alb-cre)21Mgn/J (Jackson Labs, Bar Harbor, ME) to create hepatocyte-specific *Tiparp* knock-out mice (*Tiparp*$^{tm1c/tm1c}$*Cre*^{Alb}; referred to as *Tiparp*$^{fl/fl}$*Cre*^{Alb}. This colony was maintained such that *Tiparp*$^{fl/fl}$ female mice were paired with *Tiparp*$^{fl/fl}$*Cre*^{Alb} male mice. Genotypes of all mice were determined by PCR analysis of tail biopsies using PCR primers shown in **Supplementary Table S1**. The specificity of excision events in *Tiparp*$^{fl/fl}$*Cre*^{Alb} mice was determined by quantitative real time PCR (qPCR) using primer pairs specific for exon 3 of *Tiparp* compared with primer pairs specific for intron 1 (**Supplementary Table S1**). Genotype controls used in experiments for the *Tiparp*$^{fl/fl}$*Cre*^{Alb} line are *Tiparp*$^{fl/fl}$ (observed to be phenotypically equivalent to *wild-type* (WT) mice), and for the *Tiparp*$^{Ex3-/-}$ are *Tiparp*$^{+/+}$. Both *tm1b* and *tm1d* lines were used.

In vivo dioxin treatment studies - All experiments used 8-10 week old male mice. For the acute 6 hr exposure studies, *Tiparp*$^{Ex3-/-}$ or *Tiparp*$^{fl/fl}$*Cre*^{Alb} mice and their respective strain-specific WT control mice were treated with a single intraperitoneal (i.p.) injection of 100 μg/kg dioxin, and livers were excised and flash frozen 6 hr later. For the subacute dioxin toxicity studies, mice were treated with a single i.p. injection of 10 or 100 μg/kg of dioxin and sacrificed on day 6. The 10 μg/kg dose of dioxin was dissolved in a mixture of corn oil and dimethyl sulfoxide (CO:DMSO; 90:10, referred to as CO), while the 100 μg/kg dose of dioxin was dissolved in pure DMSO. For the survival studies, mice were followed for up to 30 days after a single injection of 10 or 100 μg/kg of dioxin. Control mice received equivalent weight-adjusted volumes of CO or DMSO. The time point for euthanization was determined based on endpoint criteria for our study: a loss of 20% body weight or indications of acute distress. All control mice were euthanized to match the endpoints of dioxin-sensitive mice. For food intake studies, mice were housed individually and provided intact pellets of food that were weighed daily; a baseline was determined for each mouse by monitoring for one week prior to treatment as described previously (Ahmed, et al., 2015). Whole blood was obtained from the saphenous vein for serum alanine aminotransferase (ALT) analysis as described previously (Ahmed, et al., 2015). Hepatic glycogen levels were determined from 10 mg of frozen liver using the Glycogen Assay Kit II (Abcam). Liver, thymus, white and brown adipose tissue (WAT and BAT) were dissected and weighed. Livers from *Tiparp*$^{Ex3-/-}$ or *Tiparp*$^{fl/fl}$*Cre*^{Alb} mice treated with vehicle, 10 or 100 μg/kg dioxin were collected either on day 6 or on the day of euthanization in the survival studies. Care and treatment of animals followed the guidelines set by the Canadian Council on Animal Care, and all protocols were approved by the University of Toronto Animal Care Committee.

Hepatocytes - *Tiparp*$^{fl/fl}$*Cre*^{Alb} or *Tiparp*$^{fl/fl}$ male mice (8-10 weeks old) were used to isolate primary hepatocytes. Mouse liver was perfused with liver perfusion medium (Invitrogen) for 10 min followed by liver digestion medium for 10 min. Freshly prepared hepatocytes were seeded at a final density of 0.5×10^6 cells/well onto type I collagen coated six-well plates in attachment medium (William's E media, 10% dextran-coated charcoal (DCC) stripped fetal bovine serum (FBS), 1× penicillin/streptomycin, and 10 nM insulin). The medium was changed 2 h after plating, and all experiments were performed on the second day. Ligands were added to the cells in M199 media with 5% DCC-FBS and cells were harvested 16 h after ligand treatment for RNA extraction.

RNA extraction and gene expression analysis - Livers were removed, washed in ice-cold PBS, weighed, and flash frozen in liquid nitrogen. Frozen livers were homogenized in TRIZOL reagent (Life Technologies) and total RNA was isolated using the Aurum RNA isolation kits (BioRad) and reverse transcribed as previously described (Ahmed, et al.,

2015). Primers used to amplify target transcripts are provided in **Supplementary Table S1** or described elsewhere (Ahmed, et al., 2015). All genes were normalized to TATA binding protein (Tbp) levels and analyzed using the comparative C_T ($\Delta\Delta$ C_T) method.

ChIP assays - ChIP assays were performed as previously described (Lo *et al.*, 2011). Briefly, approximately 100 mg of frozen mouse liver was homogenized in 1% formaldehyde in PBS and incubated for 10 min at room temperature. The homogenate was centrifuged at 8,000xg for 5 min at 4°C. Pellet was washed in ice-cold PBS, centrifuged, and resuspended in 900 µL of TSEI (20 mM Tris-HCl [pH 8.0], 150 mM NaCl, 2 mM EDTA, 1% Triton X-100, 0.1% sodium dodecyl sulfate) + 1x Protease Inhibitor Cocktail (Sigma, St. Louis, MO). Samples were sonicated 10 times for 30 sec ON/30 sec OFF on the high setting using a Bioruptor (Diagenode). The supernatants were transferred to new microcentrifuge tubes and incubated with rabbit IgG (5 µg; Sigma) and anti-AHR (5 µg; SA-210, Enzo) overnight at 4°C under gentle agitation. ChIP samples were washed, the DNA and the ChIP-qPCR was performed as previously described (Lo *et al.*, 2011).

Histology – Hematoxylin and Eosin and Oil-Red-O/Hematoxylin staining were performed following standard methods with representative images provided. Paraformaldehyde-fixed or OCT-embedded tissues were provided to the Histology Core Facility at the Princess Margaret Cancer Centre, Toronto, Ontario, for all histology sample processing, staining and scanning of stained slides.

Western blotting - For hepatic AHR protein detection, whole cell extracts were prepared by homogenizing 100 mg of liver tissue in RIPA lysis buffer. Ten micrograms of total protein were separated by SDS-PAGE and transferred to a nitrocellulose membrane. Membranes were incubated with anti-AHR antibody (SA-210) and stripped and then incubated with anti-β-actin antibody (Sigma A-2228).

Metabolomics – *Tiparp*$^{fl/fl}$ and *Tiparp*$^{fl/fl}$*Cre*^{Alb} mice were treated with a single intraperitoneal injection of CO:DMSO or 10 µg/kg dioxin. Liver tissue (100 mg) was collected on day 3 and flash frozen in liquid nitrogen. The frozen tissue was extracted and metabolomic analyses were performed by Metabolon (Durham, NC). Raw data received from Metabolon were preprocessed to input missing values and normalized using logarithmic transformation. Shapiro's test was used to test for normality and Levene's test was used to test for the homogeneity of variances. ANOVA was used to analyze the differences in group means, followed by Tukey's-HSD for post-hoc correction. The FDR method was used to adjust the *p*-values for multiple ANOVA tests (one for each metabolite). At an FDR of 10%, all the group comparisons that exhibited a statistically

significant difference (post-hoc corrected p-values < 0.05) were considered significant. All the analyses were performed in R version 3.4.1.

Statistical Analysis - All data were presented as means and S.E.M. Two-way analysis of variance (ANOVA) followed by Sidak's post-hoc test or one-way ANOVA followed by Tukey's post-hoc test were used to assess statistical significance (P<0.05) using GraphPad Prism 6 Software (San Diego, CA) or R version 3.4.1.

Results

Generation of Conditional Tiparp$^{fl/fl}$ Mice – Mice harboring the conditional *Tiparp^{fl}* allele were generated from *Tiparp$^{tm1a(EUCOMM)Wtsi}$* ES cells purchased from EUCOMM. A partial map of both the *Tiparp* WT and *Tiparp tm1a* alleles is shown in **Fig. 1A**. Southern blotting of genomic DNA isolated from 4 different ES cell clones confirmed the correct integration of the tm1a allele in the ES cell clones D3 and G3 (**Fig. 1B**). Mice generated in this study were from ES cell clone G3. Mice harboring the conditional *Tiparp^{fl}* allele were generated from the *Tiparp tm1a* allele by excision of the neomycin and LacZ genes through crosses with B6(C3)-Tg(Pgk1-FLPo)10Sykr/J mice, leaving the targeted exon flanked by LoxP sites. Mice heterozygous for the tm1c allele were then intercrossed to make homozygous tm1c mice (*Tiparp$^{fl/fl}$*; *tm1c* allele).

Complete and Hepatocyte-Specific Excision of the Tiparp$^{fl/fl}$ Allele – Using genetrap targeted TIPARP null mice in which a LacZ gene is inserted in front of exon 1 in the *Tiparp* gene (Schmahl *et al.*, 2007), we reported that loss of TIPARP expression increased the sensitivity of mice to dioxin-induced steatohepatitis and lethality (Ahmed, et al., 2015). These findings supported the notion that TIPARP protects against dioxin-induced toxicity by negatively regulating AHR action. Because the type of gene knockout targeting strategy can impact the phenotypes observed from targeting the same gene, we created a complete TIPARP knockout by removal of exon 3 of *Tiparp* (*Tiparp$^{Ex3-/-}$*) as described in Materials and Methods. To generate a complete TIPARP null mouse in which exon 3 is removed (*Tiparp$^{Ex3-/-}$*) we used two different strategies. In the first approach, mice heterozygous for the tm1c allele were bred to B6.C-Tg(CMV-cre)1Cgn/J mice to remove the targeted exon (*Tiparp$^{Ex3-/-}$*; tm1d allele). In second approach, mice carrying the tm1a allele were bred to B6.C-Tg(CMV-cre)1Cgn/J mice to remove the Neo cassette and the targeted exon and leave the lacZ reporter (*Tiparp$^{Ex3-/-}$*; *tm1b* allele). A map of the *Tiparp tm1c*, *tm1d* and *tm1b* alleles is shown in **Fig. 1C**. The correct genotype was confirmed by PCR analysis of genomic DNA (**Fig. 1D**). *Tiparp$^{Ex3-/-}$* mice represent a distinct TIPARP null strain compared with *Tiparp* targeted knockout using a genetrap approach (Ahmed, et al., 2015; Schmahl, et al., 2007). To determine whether the loss of TIPARP in hepatocytes is sufficient to increase sensitivity to dioxin-dependent toxicity,

we generated mice in which *Tiparp* was deleted in hepatocytes, *Tiparp*$^{fl/fl}$*Cre*^{Alb} (**Fig. 2A**). *Tiparp*$^{fl/fl}$*Cre*^{Alb} mice were created by breeding mice homozygous for the tm1c allele (*Tiparp*$^{fl/fl}$) with B6N.Cg-Tg(Alb-cre)21Mgn/J mice to remove the targeted exon specifically in hepatocytes (Walisser, et al., 2005). For the *Tiparp*$^{fl/fl}$*Cre*^{Alb} line, WT mice were referred to as *Tiparp*$^{fl/fl}$, whereas for the *Tiparp*$^{Ex3-/-}$ line, WT mice were referred to as *Tiparp*$^{+/+}$ for simplicity.

To examine the specificity of excision events in *Tiparp*$^{fl/fl}$*Cre*^{Alb} mice, we analyzed various tissues by determining the relative ratios of *Tiparp* exon 3 compared with intron 1 using qPCR. *Tiparp* exon 3 was efficiently excised in liver tissue and in isolated hepatocytes (Hepa) in the presence of Cre^{Alb}, but not in the other tissues examined (**Fig. 2A**). *Tiparp* exon 3 was not detected in liver tissue isolated from *Tiparp*$^{Ex3-/-}$ mice (**Fig. 2B**). In the absence of Cre^{Alb}, the *Tiparp*$^{fl/fl}$ mice showed only the *Tiparp*^{fl}-unexcised allele in all tissues and isolated hepatocytes examined (**Fig. 2A**).

Cloning and DNA sequencing revealed that the conditional inactivation of the *Tiparp*^{fl} allele accomplished by Cre-mediated deletion of exon 3 (169 bp) results in splicing and fusion between exon 2 (961 bp) and exon 4 (161 bp), leading to the insertion of a premature stop codon. This truncated version of TIPARP contains 311 amino acids, of which the last 4 are the result of a frameshift (the full-length protein is 657 a.a.), and it lacks its WWE and catalytic domains (MacPherson, et al., 2013). In agreement with a previous study, cloning and transient transfection of the truncated TIPARP protein failed to inhibit AHR-dependent and dioxin-induced CYP1A1 reporter gene activity (**Supplementary Fig. S1**).

Consistent with TIPARP's role as a negative regulator of AHR activity, exposure of hepatocytes from *Tiparp*$^{fl/fl}$*Cre*^{Alb} mice for 6 hr to 10 nM dioxin increased mRNA expression levels of the AHR target genes *Cyp1a1, Cyp1a2* and *Cyp1b1* compared with similarly treated hepatocytes from *Tiparp*$^{fl/fl}$ mice (**Fig. 2C**). *Tiparp* mRNA expression levels were markedly decreased in hepatocytes isolated from *Tiparp*$^{fl/fl}$*Cre*^{Alb} mice compared with *Tiparp*$^{fl/fl}$ mice. We next examined the effect of TIPARP loss on AHR target gene expression in liver and lung tissues isolated from *Tiparp*$^{Ex3-/-}$, *Tiparp*$^{fl/fl}$*Cre*^{Alb} and WT mice 6 h after treatment with 100 μg/kg dioxin. Higher *Cyp1a1* and *Cyp1b1* mRNA levels were observed in both liver and lung from *Tiparp*$^{Ex3-/-}$ mice than in *Tiparp*$^{Ex3+/+}$ mice (**Fig. 3A and B**). *Tiparp* mRNA levels were not detected in liver or lung from *Tiparp*$^{Ex3-/-}$ mice compared with *Tiparp*$^{+/+}$ mice (**Fig. 3C**). Significantly increased dioxin-induced *Cyp1a1* and *Cyp1b1* mRNA levels above those observed in *Tiparp*$^{fl/fl}$ mice were only observed in liver and lung from *Tiparp*$^{fl/fl}$*Cre*^{Alb} mice (**Fig. 3D and E**). As expected, TIPARP expression levels were reduced in liver, but not in lung in *Tiparp*$^{fl/fl}$*Cre*^{Alb} compared with *Tiparp*$^{fl/fl}$ mice (**Fig. 3F**).

Tiparp*$^{Ex3-/-}$ *Mice Exhibit Increased Sensitivity to Dioxin-Induced Toxicity and Lethality – To determine the sensitivity of *Tiparp*$^{Ex3-/-}$ mice to dioxin-induced toxicity,

these mice and their respective WT controls were injected with a single dose of 10 or 100 μg/kg dioxin and monitored for up to 30 days, as previously described (Ahmed, et al., 2015). All *Tiparp*$^{Ex3+/+}$ mice were normal in physical appearance at the end of the 30-day observation period (**Fig. 4A**), while no dioxin-treated *Tiparp*$^{Ex3-/-}$ mice (tm1d or tm1b) survived the 30-day experiment (**Fig. 4A**). *Tiparp*$^{Ex3-/-}$ mice treated with 100 μg/kg dioxin became weakened and moribund and were humanely euthanized between days 2 and 3, while those treated with 10 μg/kg dioxin were euthanized at day 7. *Tiparp*$^{Ex3-/-}$ mice treated with 10 μg/kg dioxin had lost significant body weight by 5 days after treatment (**Fig. 4B**); however, no decrease in food intake was observed (**Fig. 4C**). No changes in food intake or body weight were seen in dioxin-exposed *Tiparp*$^{+/+}$ mice. Serum ALT activity, a marker of hepatotoxicity, was significantly increased in dioxin-treated *Tiparp*$^{Ex3-/-}$ mice, while no increase above controls was observed in *Tiparp*$^{+/+}$ mice (**Fig. 4D**). Increased liver weight was observed in dioxin-treated *Tiparp*$^{+/+}$ mice but not in *Tiparp*$^{Ex3-/-}$ mice (**Fig. 4E**). Thymic involution, an endpoint associated with dioxin toxicity, responded as expected in both genotypes at day 7 (**Fig. 4F**). A significant decrease in epididymal white adipose tissue (WAT) weight was seen in *Tiparp*$^{Ex3-/-}$ mice but not in WT mice **(Fig. 4G)**. No differences in brown adipose tissue (BAT) weight were observed (data not shown). Hepatic glycogen stores were lower in dioxin-treated *Tiparp*$^{Ex3-/-}$ mice than in WT mice **(Fig. 4H)**. These data support the importance of TIPARP in regulating AHR action and show that loss of its expression in mice increases their sensitivity to dioxin toxicity.

Hepatocyte-Specific Loss of TIPARP Results in Increased Sensitivity to Dioxin-Induced Toxicity and Lethality – Because AHR expression in hepatocytes is required for dioxin-induced liver toxicity, we hypothesized that the loss of TIPARP expression in hepatocytes would enhance dioxin-dependent liver toxicity. To test this hypothesis, we treated *Tiparp*$^{fl/fl}$*Cre*^{Alb} and *Tiparp*$^{fl/fl}$ mice with a single i.p. injection of 10 or 100 μg/kg dioxin and monitored the mice for up to 30 days. As expected, all *Tiparp*$^{fl/fl}$ mice were normal in physical appearance at the end of the 30-day observation period (**Fig. 5A**). No dioxin-treated *Tiparp*$^{fl/fl}$*Cre*^{Alb} mice survived the 30-day experiment (**Fig. 5A**). *Tiparp*$^{fl/fl}$*Cre*^{Alb} mice treated with 100 μg/kg dioxin appeared weakened and moribund and were humanely euthanized between day 3 and 5, while those treated with 10 μg/kg dioxin were humanely euthanized at day 9. Sensitivity to dioxin-induced lethality was significantly different between *Tiparp*$^{fl/fl}$*Cre*^{Alb} and *Tiparp*$^{Ex3-/-}$ mice at both 10 and 100 μg/kg dioxin, suggesting that cells other than hepatocytes also contribute to dioxin lethality in these models. *Tiparp*$^{fl/fl}$*Cre*^{Alb} mice treated with 10 μg/kg dioxin had lost significant body weight by 6 days after treatment (**Fig. 5B**), while no decrease in food intake was observed (**Fig. 5C**). No change in food intake or body weight was seen in *Tiparp*$^{fl/fl}$ mice. Serum ALT was significantly increased in dioxin-treated *Tiparp*$^{fl/fl}$*Cre*^{Alb} mice at days 3 and 6, but no increase was observed in *Tiparp*$^{fl/fl}$ mice (**Fig. 5D**). Increased

liver weight was observed in dioxin-treated *Tiparp*$^{fl/fl}$ mice but not in *Tiparp*$^{fl/fl}$*Cre*^{Alb} mice (**Fig. 5E**). Decreased thymus weight was seen in both genotypes at day 9 (**Fig. 5F**). Consistent with dioxin-treated *Tiparp*$^{Ex3-/-}$ mice, *Tiparp*$^{fl/fl}$*Cre*^{Alb} mice had significantly decreased epididymal WAT levels compared with WT mice **(Fig. 5G)**. No difference in BAT weight was observed (data not shown). Hepatic glycogen stores were also decreased in dioxin-treated *Tiparp*$^{fl/fl}$*Cre*^{Alb} mice compared with *Tiparp*$^{fl/fl}$ mice **(Fig. 5H)**. These findings show that hepatocyte-specific deletion of TIPARP is sufficient to increase dioxin-induced toxicity and lethality.

As an independent measure of liver toxicity, livers were sectioned and stained with hematoxylin and eosin. Vehicle-treated *Tiparp*$^{fl/fl}$ and *Tiparp*$^{fl/fl}$*Cre*^{Alb} mice had histologically normal liver architecture (**Fig. 6A**). On day 9, dioxin-treated *Tiparp*$^{fl/fl}$ livers exhibited slight hepatocyte cytoplasmic clearing within periportal regions and inflammatory cell infiltration (**Fig. 6A**). In contrast, day 9 *Tiparp*$^{fl/fl}$*Cre*^{Alb} livers were characterized by inflammatory infiltration and a predominant microvesicular steatosis. Six days after dioxin treatment, livers from *Tiparp*$^{fl/fl}$ mice displayed distinct inflammatory cell infiltration and increased clearing of the cytoplasm with the appearance of large vacuoles within hepatocytes. Similar findings were observed in livers isolated from dioxin-treated *Tiparp*$^{+/+}$ and *Tiparp*$^{Ex3-/-}$ mice (**Supplementary Fig. 2A)**.

We next determined the mRNA levels of AHR-regulated cytokines and the macrophage marker F4/80 (Casado *et al.*, 2011; Matsubara *et al.*, 2012). Hepatic interleukin 6 (*Il6*) levels were unaffected by dioxin treatment in both genotypes (**Fig. 6B**). However, dioxin-treated *Tiparp*$^{fl/fl}$*Cre*^{Alb} mice had increased hepatic expression of *Serpine 1* (also known as plasminogen activator inhibitor-1; PAI-1), chemokine (C-X-C motif) ligand 2 (*Cxcl2*) and *F4/80* when compared with *Tiparp*$^{fl/fl}$ mice (**Fig 6C-E**). Similar findings were also seen in livers isolated from dioxin-treated *Tiparp*$^{+/+}$ and *Tiparp*$^{Ex3-/-}$ mice (**Supplementary Fig. 2B-E)**. The increased cytokine and F4/80 levels increased hepatic inflammation in dioxin-treated *Tiparp*$^{fl/fl}$*Cre*^{Alb} compared with wild-type mice.

Hepatocyte-Specific Loss of TIPARP Increases Dioxin-Induced Steatohepatitis - Livers from vehicle-treated *Tiparp*$^{fl/fl}$ and *Tiparp*$^{fl/fl}$*Cre*^{Alb} mice were macroscopically normal (**Fig. 7A**). Livers from *Tiparp*$^{fl/fl}$ mice were enlarged but only slightly pale in color 9 days after dioxin treatment (**Fig. 7A**). Livers from dioxin-treated *Tiparp*$^{fl/fl}$*Cre*^{Alb} mice were markedly pale in color at 9 days, suggesting a high level of lipid accumulation. We tested for the presence of neutral lipids by Oil-Red-O staining (**Fig. 7B**). Livers from vehicle-exposed *Tiparp*$^{fl/fl}$ and *Tiparp*$^{fl/fl}$*Cre*^{Alb} mice were negative for Oil-Red-O staining. On day 9 after dioxin treatment, small droplets of lipid were seen in the livers of *Tiparp*$^{fl/fl}$ mice, while those from similarly treated *Tiparp*$^{fl/fl}$*Cre*^{Alb} mice had substantial intracytoplasmic lipid accumulation. Comparable findings were observed in livers isolated from dioxin-treated *Tiparp*$^{+/+}$ and *Tiparp*$^{Ex3-/-}$ mice (**Supplementary Fig. 3A & B)**.

We then analyzed the hepatic levels of transcripts encoding genes involved in lipid uptake, lipogenesis and cholesterol/bile acid metabolism. Consistent with previous studies (Lee, et al., 2010; Lu *et al.*, 2011), the lipid uptake transporter, scavenger receptor encoded by cluster of differentiation 36 (*Cd36*), was increased 3-fold by dioxin treatment in *Tiparp*$^{fl/fl}$ mice and to a greater extent (8-fold) in similarly treated *Tiparp*$^{fl/fl}$*Cre*^{Alb} mice (**Fig. 7C**). Hepatic expression of lipogenic genes including sterol regulatory element-binding transcription factor 1 (*Srebp1*), and stearoyl-CoA desaturase (*Scd1*) were significantly decreased in dioxin treated *Tiparp*$^{fl/fl}$*Cre*^{Alb} mice compared with *Tiparp*$^{fl/fl}$ mice (**Fig. 7D & E**). Peroxisome proliferator activating receptor α (*Ppara*) and *Cyp7a1*, the rate limiting enzyme bile acid synthesis, were also significantly decreased in *Tiparp*$^{fl/fl}$*Cre*^{Alb} mice compared with *Tiparp*$^{fl/fl}$ mice (**Fig. 7F-G**). Similar findings were seen in livers isolated from dioxin-treated *Tiparp*$^{+/+}$ and *Tiparp*$^{Ex3-/-}$ mice (**Supplementary Fig. 3C-G)**. These data suggest that the increased sensitivity of *Tiparp*$^{fl/fl}$*Cre*^{Alb} and *Tiparp*$^{Ex3-/-}$ mice to dioxin-induced steatohepatitis is due to increased lipid uptake rather than increased hepatic lipogenesis.

Increased AHR Regulated Gene Expression in Tiparp*$^{fl/fl}$*Cre*^{Alb} *Mice after Treatment with 10 μg/kg Dioxin – To identify AHR genes and/or changes in metabolites that might provide insight into the molecular mechanisms regulating the increased dioxin sensitivity of *Tiparp*$^{fl/fl}$*Cre*^{Alb} mice, we analyzed changes in dioxin-induced hepatic mRNA and metabolite levels 3 days after dioxin treatment. Day 3 was chosen because we observed significant increases in serum ALT activity in *Tiparp*$^{fl/fl}$*Cre*^{Alb} mice, and we reasoned that this time point could be used to identify early changes in AHR target gene expression and/or metabolite levels prior to more severe toxicities that ultimately led to death. *Tiparp*$^{fl/fl}$*Cre*^{Alb} mice treated with 10 μg/kg dioxin exhibited increased mRNA expression levels of many AHR target genes including *Cyp1a1, Cyp1a2, Ahrr, Nqo1, Nfe2l2* and *Serpine1* compared with similarly treated *Tiparp*$^{fl/fl}$ mice (**Fig. 8 A, C-H**). *Cyp1a2* expression was slightly increased in *Tiparp*$^{fl/fl}$*Cre*^{Alb} compared with *Tiparp*$^{fl/fl}$ mice, but this difference was not statistically significant (**Fig. 8B**). No significant increase in AHR recruitment to *Cyp1a1* was observed (**Fig. 8I**). Significantly higher levels of AHR were recruited to *Cyp1b1* in liver extracts from *Tiparp*$^{fl/fl}$*Cre*^{Alb} mice compared with *Tiparp*$^{fl/fl}$ mice (**Fig. 8J**). Consistent with our previous study, we observed reduced dioxin-induced proteolytic degradation of total AHR protein in liver extracts from *Tiparp*$^{fl/fl}$*Cre*^{Alb} mice compared with *Tiparp*$^{fl/fl}$ mice (**Fig. 8K**).

We next did comparative metabolomic analyses on liver extracts from *Tiparp*$^{fl/fl}$*Cre*^{Alb} and *Tiparp*$^{fl/fl}$ mice. Principal component analysis (PCA) revealed significant treatment-based separations among the samples, with clear distinctions between the vehicle- and dioxin-treated animals in each genotype. Separations were also apparent between the dioxin-treated *Tiparp*$^{fl/fl}$ and *Tiparp*$^{fl/fl}$*Cre*^{Alb} animals (**Fig. 9A**). Of the total of 679 named metabolites examined, 213 were significantly altered ($P<0.05$) by

dioxin treatment of *Tiparp*$^{fl/fl}$*Cre*^{Alb} mice compared with 124 in similarly treated *Tiparp*$^{fl/fl}$ mice (**Table 1**; **Supplementary Tables S2 & S3**). Of the 124 metabolites, 74 overlapped with those identified in dioxin-treated *Tiparp*$^{fl/fl}$*Cre*^{Alb} mice (**Fig. 9B**). Only 7 metabolites were significantly changed in vehicle-treated *Tiparp*$^{fl/fl}$*Cre*^{Alb} compared with *Tiparp*$^{fl/fl}$ mice, showing that the loss of TIPARP had little effect on basal liver metabolism (**Supplementary Tables S4**). Consistent with previous studies, dioxin treatment resulted in significant lipidomic changes, with accumulation of several classes of free fatty acids and metabolites linked to complex lipid homeostasis (Nault *et al.*, 2016b). Increased lipids were observed in both the *Tiparp*$^{fl/fl}$ and *Tiparp*$^{fl/fl}$*Cre*^{Alb} animals, with a few classes of lipids that were differentially expressed in the two groups (**Supplementary Table S2 and S3**). These included certain long-chain acylcarnitines, fatty acid dicarboxylates, and complex lipids such as plasmalogens and sphingolipids. However, 129 metabolites were altered in dioxin-treated *Tiparp*$^{fl/fl}$*Cre*^{Alb} compared with *Tiparp*$^{fl/fl}$ mice (**Table 1; Supplementary Table S5**). Altered metabolite levels in *Tiparp*$^{fl/fl}$*Cre*^{Alb} and *Tiparp*$^{fl/fl}$ mice were analyzed for pathway over-representation (enrichment) and connectivity within related metabolites (impact) using MetaboAnalyst (Xia *et al.*, 2016) (**Fig. 9C & D**). Only glycerophospholipid metabolism was common among the top 5 or 6 significant pathways (**Supplementary Tables S6 and S7**). Dioxin-treated *Tiparp*$^{fl/fl}$*Cre*^{Alb} mice also differed with regard to increased γ-glutamyl-ε-lysine levels (12.5-fold; **Fig 9E**), which may reflect increased transglutaminase activity, and polyamine metabolism (*N*-acetylputrescine; **Fig 9F**, and putrescine; **Fig. 9G**). Because dioxin toxicity has been tightly linked with NAD^+ levels, its precursors and metabolites, and because TIPARP activity is dependent on NAD^+, we examined NAD^+ metabolism (Diani-Moore *et al.*, 2010; Diani-Moore *et al.*, 2017; He *et al.*, 2013). Dioxin-dependent increases in nicotinamide ribonucleoside (**Fig. 9H**) and nicotinamide (**Fig 9I**) were observed in *Tiparp*$^{fl/fl}$*Cre*^{Alb} and *Tiparp*$^{fl/fl}$ mice, respectively. Significant decreases in intrahepatic NAD^+ levels were only observed in dioxin-treated *Tiparp*$^{fl/fl}$*Cre*^{Alb} mice (**Fig. 9J**).

Discussion

We previously reported that TIPARP acts as part of negative feedback loop to regulate AHR activity, and that global loss of TIPARP expression increases sensitivity to dioxin-induced toxicities such as steatohepatitis and wasting syndrome (Ahmed, et al., 2015; MacPherson, et al., 2013). Since hepatocyte-specific deletion of AHR prevents dioxin-induced hepatotoxicity, we reasoned that hepatocyte-specific deletion of TIPARP would result in increased dioxin-induced hepatotoxicity. We therefore generated a hepatocyte-specific TIPARP deletion (*Tiparp*$^{fl/fl}$*Cre*^{Alb}) mouse strain. We also generated a whole-body knockout TIPARP (*Tiparp*$^{Ex3-/-}$) strain in which *Tiparp* is deleted by the removal of exon 3, making it distinct from other TIPARP null lines (Ahmed, et al., 2015; Kozaki *et al.*, 2017; Schmahl, et al., 2007). Here we show that *Tiparp*$^{Ex3-/-}$ and *Tiparp*$^{fl/fl}$*Cre*^{Alb} mice are both more sensitive than WT mice to dioxin-induced hepatotoxicity and lethality. These findings provide further support for the importance of

TIPARP in AHR signaling and for its role in protecting against dioxin-induced toxicity (Ahmed, et al., 2015; Matthews, 2017), as well as demonstrating that the expression of TIPARP in hepatocytes plays a key role in the manifestations of this toxicity.

Tiparp$^{fl/fl}$*Cre*^{Alb} mice treated with dioxin lost significant body weight without any reduction in food intake. Hepatic glycogen and epididymal WAT levels were also reduced, pointing to a possible deficiency in the efficiency of intestinal nutrient absorption resulting in altered metabolism. Dioxin-induced hypophagia contributes to body weight and adipose tissue loss in many species, but numerous studies using pair-feeding or total parenteral nutrition have failed to identify a single explanation for the weight loss (Linden, et al., 2010; Seefeld, et al., 1984). The severe hepatotoxicity and extensive hepatosteatosis in dioxin-treated *Tiparp*$^{fl/fl}$*Cre*^{Alb} and *Tiparp*$^{Ex3-/-}$ mice, would cause impaired liver function that could result in reduced intestinal nutrient absorption and impaired liver homeostasis (Kalaitzakis, 2014).

Dioxin-treated *Tiparp*$^{fl/fl}$*Cre*^{Alb} and *Tiparp*$^{Ex3-/-}$ mice exhibit many of the alterations in lipid homeostasis, increased hepatic inflammation and other toxic endpoints that have been reported in other studies (Boverhof *et al.*, 2006; Duval *et al.*, 2017). *Tiparp*$^{fl/fl}$*Cre*^{Alb} and *Tiparp*$^{Ex3-/-}$ mice exhibited increased hepatosteatosis due to increased expression of genes regulating lipid uptake (*Cd36*), but decreased expression of those involved in fatty acid β-oxidation and *de novo* lipogenesis (*Scd1, Srebp1, Ppara*) (Ahmed, et al., 2015; Duval, et al., 2017; Lee, et al., 2010). *Scd1* expression was increased in *Tiparp*$^{fl/fl}$ mice, but decreased in *Tiparp*$^{fl/fl}$*Cre*^{Alb} mice. One possible explanation is that the increased hepatosteatosis in *Tiparp*$^{fl/fl}$*Cre*^{Alb} mice results in negative regulation of *Scd1* by other factors or hormones (Mauvoisin *et al.*, 2011). *Srebp1* expression levels were decreased in *Tiparp*$^{fl/fl}$*Cre*^{Alb} and *Tiparp*$^{Ex3-/-}$ mice, supporting findings from a recent high-dose dioxin exposure study (Duval, et al., 2017). *Srebp1* expression is positively regulated by the liver X receptor (LXR) and PPARα. TIPARP is an LXR coactivator, so the loss of *Tiparp* expression combined with the reduced PPARα expression levels could also contribute to reduced SREBP1 levels (Bindesboll *et al.*, 2016).

CYP7A1 plays a critical role in the control of bile acid and cholesterol homeostasis as the rate-limiting enzyme in the classic bile acid synthesis pathway (Gupta *et al.*, 2001). Overexpression of mouse CYP7A1 protects against high-fat diet induced obesity, fatty liver and insulin resistance (Li *et al.*, 2010), whereas in humans, genetic deficiency of CYP7A1 leads to hyperlipidemia (Pullinger *et al.*, 2002). The decrease in CYP7A1 expression levels in treated *Tiparp*$^{fl/fl}$*Cre*^{Alb} and *Tiparp*$^{Ex3-/-}$ mice is in agreement with studies of male C57BL/6 mice treated with 0.01 to 30 μg/kg dioxin every 4 days for 28 days (Fader *et al.*, 2017), and could be a contributing factor to the increased hepatosteatosis and reduced WAT levels observed, through reduced lipid absorption resulting from altered bile acid homeostasis (Fader, et al., 2017). In support of this, we

observed increased hepatic levels of taurochenodeoxycholic acid and taurocholic acid in dioxin-treated *Tiparp*$^{fl/fl}$*Cre*^{Alb} mice but not in *Tiparp*$^{fl/fl}$ mice.

Metabolomic profiling studies identified significant changes in metabolite levels in dioxin-treated *Tiparp*$^{fl/fl}$*Cre*^{Alb} mice compared with *Tiparp*$^{fl/fl}$ mice. Many of the major treatment-based changes were conserved in the two cohorts (*i.e.,* accumulated fatty acids, changes related to nucleotides and polyamines). However, the extent of change of the affected metabolites differed between the *Tiparp*$^{fl/fl}$ and *Tiparp*$^{fl/fl}$*Cre*^{Alb} groups. Dioxin-treated *Tiparp*$^{fl/fl}$*Cre*^{Alb} mice, however, exhibited significant increases in gamma-glutamyl-epsilon lysine levels compared with their untreated counterparts or dioxin-treated *Tiparp*$^{fl/fl}$ mice. This metabolite is formed by tissue transglutaminase (TG2), which catalyzes crosslinks between glutamine and lysine residues of proteins (Iismaa *et al.*, 2009). TG2 activity increases following acute and chronic liver injury, and aberrant TG2 activation has been implicated in the development of fibrosis and cancer (Iismaa, et al., 2009). In contrast, retinoid-induced TG2 mRNA up-regulation is reduced by dioxin treatment in a human squamous cell carcinoma cell line (Krig *et al.*, 2000). The increased γ-glutamyl-ε-lysine observed in *Tiparp*$^{fl/fl}$*Cre*^{Alb} mice suggests that TIPARP might influence TG2 activity following dioxin-induced liver damage.

We observed that the expression of most of the AHR target genes examined was increased in response to dioxin in *Tiparp*$^{fl/fl}$*Cre*^{Alb} and *Tiparp*$^{fl/fl}$ compared with WT mice, including *Cxcl2* (macrophage inflammation protein-2) and *Serpine1* genes (Son *et al.*, 2002). CXCL2 is a member of the CXC subfamily of chemokines that are crucial for neutrophil recruitment to sites of inflammation following hepatic injury (Marra *et al.*, 2014). Levels of plasminogen activator inhibitor-1 (PAI-1), the product of *Serpine1* gene, were higher in *Tiparp*$^{fl/fl}$*Cre*^{Alb} mice than in *Tiparp*$^{fl/fl}$ mice. PAI-1 is a physiologic inhibitor of plasminogen activators that regulate fibrosis via regulation of the extracellular matrix. PAI-1 expression is increased in dioxin-induced fibrosis (Nault *et al.*, 2016a).

The mRNA levels of AHR repressor (AHRR), a negative regulator of AHR (Mimura *et al.*, 1999), were increased in *Tiparp*$^{fl/fl}$*Cre*^{Alb} compared with *Tiparp*$^{fl/fl}$ mice. AHRR is a potent inhibitor of AHR activity *in vitro* (Karchner *et al.*, 2009) that exhibits gene- and tissue-specific inhibition of AHR signaling in mice (Hosoya *et al.*, 2008). Although the effect of *Ahrr* loss on dioxin-induced wasting syndrome has not been reported, AHRR transgenic mice are protected from dioxin-induced lethality and hepatotoxicity (Vogel et al., 2016).

Increased TIPARP and PARP1 activity have been proposed to be important in augmenting dioxin toxicity through the depletion of NAD^+. Indeed, NAD^+ repletion or treatment with the pan-PARP inhibitor PJ34 can prevent dioxin-induced thymic atrophy and hepatosteatosis in a chicken embryo model (Diani-Moore, et al., 2017). However, we observed decreased hepatic NAD^+ levels in dioxin-treated *Tiparp*$^{fl/fl}$*Cre*^{Alb} mice, suggesting that PARP1 or an NAD^+-consuming enzyme other than TIPARP is

responsible for the reduced NAD^+ levels after dioxin treatment in mice. Another possible explanation is that there are species differences in the AHR-TIPARP signaling axis, such that TIPARP protects against dioxin toxicity in mice but enhances it in avian species. Further studies using gene targeting methods to delete TIPARP in non-murine models are needed to explain these discrepancies.

AHR is also a key regulator of gut homeostasis, inflammation, immunity and T cell differentiation (Stockinger *et al.*, 2014). AHR is required for the maintenance of intraepithelial lymphocytes (IELs), which are the first line of immune defense in the intestine. Loss of AHR or reduced exposure to dietary AHR ligands compromises these cells, leading to increased microbial load, immune activation and epithelial damage (Li *et al.*, 2011). Moreover, AHR activation by dietary indoles (indole-3-carbinol) improves colitis and protects against experimental autoimmune encephalomyelitis (EAE), a murine model of multiple sclerosis (MS) (Lamas *et al.*, 2016; Li, et al., 2011; Monteleone *et al.*, 2011; Rouse *et al.*, 2013). An unanswered question is whether TIPARP also regulates endogenous AHR signaling and if so, how would its loss affect the protective role of the AHR signaling pathway in models of inflammatory disease? Kynurenine, an endogenous AHR ligand, was reported to repress type-I-IFN responses during viral infection in an AHR- and TIPARP-dependent manner, supporting the notion that TIPARP has a broad role in AHR biology and regulates endogenous ligand-induced AHR activation (Yamada *et al.*, 2016).

In summary, we provide evidence from two additional mouse models that the loss of TIPARP expression increases sensitivity to dioxin toxicity and lethality. Hepatocyte-specific loss of TIPARP is sufficient to increase sensitivity to dioxin hepatotoxicity, steatosis and lethality, highlighting the importance of liver damage in the dioxin-induced wasting syndrome. Our results provide further support for the importance of the AHR-TIPARP axis in regulating dioxin toxicity, and potentially in regulating the biological actions of AHR following its activation by endogenous or dietary ligands.

Funding Information

This work was supported by Canadian Institutes of Health Research (CIHR) operating grants (MOP-494265 and MOP-125919), CIHR New Investigator Award, an Early Researcher Award from the Ontario Ministry of Innovation (ER10-07-028), an unrestricted research grant from the DOW Chemical Company, the Johan Throne Holst Foundation, Novo Nordic Foundation and the Norwegian Cancer Society to J.M.

Acknowledgements

The authors thank all members of the Matthews and Grant laboratories for their help with the preparation of the manuscript.

Declaration of Interest

The authors have nothing to declare.

Supplemental Data

Data available from the Dryad Digital Repository https://doi.org/10.5061/dryad.rc5b58m

References

Ahmed, S., Bott, D., Gomez, A., Tamblyn, L., Rasheed, A., MacPherson, L., Sugamori, K. S., Cho, T., Yang, Y., Grant, D. M., *et al.* (2015). Loss of the Mono-ADP-Ribosyltransferase, TIPARP, Increases Sensitivity to Dioxin-Induced Steatohepatitis and Lethality. *J Biol Chem* **290**(27), 16824-40.

Bindesboll, C., Tan, S., Bott, D., Cho, T., Tamblyn, L., MacPherson, L., Gronning-Wang, L. M., Nebb, H. I., and Matthews, J. (2016). TCDD-inducible poly-ADP-ribose polymerase (TIPARP/PARP7) mono-ADP-ribosylates and coactivates liver X receptors. *Biochem J* **473**(7), 899-910.

Birnbaum, L. S. (1994). Endocrine effects of prenatal exposure to PCBs, dioxins, and other xenobiotics: implications for policy and future research. *Environ Health Perspect* **102**(8), 676-9.

Birnbaum, L. S. (1995). Developmental effects of dioxins and related endocrine disrupting chemicals. *Toxicol Lett* **82-83**, 743-50.

Boverhof, D. R., Burgoon, L. D., Tashiro, C., Sharratt, B., Chittim, B., Harkema, J. R., Mendrick, D. L., and Zacharewski, T. R. (2006). Comparative toxicogenomic analysis of the hepatotoxic effects of TCDD in Sprague Dawley rats and C57BL/6 mice. *Toxicol Sci* **94**(2), 398-416.

Casado, F. L., Singh, K. P., and Gasiewicz, T. A. (2011). Aryl hydrocarbon receptor activation in hematopoietic stem/progenitor cells alters cell function and pathway-specific gene modulation reflecting changes in cellular trafficking and migration. *Mol Pharmacol* **80**(4), 673-82.

Denison, M. S., and Nagy, S. R. (2003). Activation of the aryl hydrocarbon receptor by structurally diverse exogenous and endogenous chemicals. *Annu Rev Pharmacol Toxicol* **43**, 309-34.

Diani-Moore, S., Ram, P., Li, X., Mondal, P., Youn, D. Y., Sauve, A. A., and Rifkind, A. B. (2010). Identification of the aryl hydrocarbon receptor target gene TiPARP as a mediator of suppression of hepatic gluconeogenesis by 2,3,7,8-tetrachlorodibenzo-p-dioxin and of nicotinamide as a corrective agent for this effect. *J Biol Chem* **285**(50), 38801-10.

Diani-Moore, S., Shoots, J., Singh, R., Zuk, J. B., and Rifkind, A. B. (2017). NAD(+) loss, a new player in AhR biology: prevention of thymus atrophy and hepatosteatosis by NAD(+) repletion. *Sci Rep* **7**(1), 2268.

Duval, C., Teixeira-Clerc, F., Leblanc, A. F., Touch, S., Emond, C., Guerre-Millo, M., Lotersztajn, S., Barouki, R., Aggerbeck, M., and Coumoul, X. (2017). Chronic

Exposure to Low Doses of Dioxin Promotes Liver Fibrosis Development in the C57BL/6J Diet-Induced Obesity Mouse Model. *Environ Health Perspect* **125**(3), 428-436.

Fader, K. A., Nault, R., Zhang, C., Kumagai, K., Harkema, J. R., and Zacharewski, T. R. (2017). 2,3,7,8-Tetrachlorodibenzo-p-dioxin (TCDD)-elicited effects on bile acid homeostasis: Alterations in biosynthesis, enterohepatic circulation, and microbial metabolism. *Sci Rep* **7**(1), 5921.

Fernandez-Salguero, P. M., Hilbert, D. M., Rudikoff, S., Ward, J. M., and Gonzalez, F. J. (1996). Aryl-hydrocarbon receptor-deficient mice are resistant to 2,3,7,8-tetrachlorodibenzo-p-dioxin-induced toxicity. *Toxicol Appl Pharmacol* **140**(1), 173-9.

Gupta, S., Stravitz, R. T., Dent, P., and Hylemon, P. B. (2001). Down-regulation of cholesterol 7alpha-hydroxylase (CYP7A1) gene expression by bile acids in primary rat hepatocytes is mediated by the c-Jun N-terminal kinase pathway. *J Biol Chem* **276**(19), 15816-22.

He, J., Hu, B., Shi, X., Weidert, E. R., Lu, P., Xu, M., Huang, M., Kelley, E. E., and Xie, W. (2013). Activation of the aryl hydrocarbon receptor sensitizes mice to nonalcoholic steatohepatitis by deactivating mitochondrial sirtuin deacetylase Sirt3. *Mol Cell Biol* **33**(10), 2047-55.

Hosoya, T., Harada, N., Mimura, J., Motohashi, H., Takahashi, S., Nakajima, O., Morita, M., Kawauchi, S., Yamamoto, M., and Fujii-Kuriyama, Y. (2008). Inducibility of cytochrome P450 1A1 and chemical carcinogenesis by benzo[a]pyrene in AhR repressor-deficient mice. *Biochem Biophys Res Commun* **365**(3), 562-7.

Hottiger, M. O., Hassa, P. O., Luscher, B., Schuler, H., and Koch-Nolte, F. (2010). Toward a unified nomenclature for mammalian ADP-ribosyltransferases. *Trends Biochem Sci* **35**(4), 208-19.

Iismaa, S. E., Mearns, B. M., Lorand, L., and Graham, R. M. (2009). Transglutaminases and disease: lessons from genetically engineered mouse models and inherited disorders. *Physiol Rev* **89**(3), 991-1023.

Kalaitzakis, E. (2014). Gastrointestinal dysfunction in liver cirrhosis. *World J Gastroenterol* **20**(40), 14686-95.

Karchner, S. I., Jenny, M. J., Tarrant, A. M., Evans, B. R., Kang, H. J., Bae, I., Sherr, D. H., and Hahn, M. E. (2009). The active form of human aryl hydrocarbon receptor (AHR) repressor lacks exon 8, and its Pro 185 and Ala 185 variants repress both AHR and hypoxia-inducible factor. *Mol Cell Biol* **29**(13), 3465-7

Kozaki, T., Komano, J., Kanbayashi, D., Takahama, M., Misawa, T., Satoh, T., Takeuchi, O., Kawai, T., Shimizu, S., Matsuura, Y.*, et al.* (2017). Mitochondrial damage elicits a TCDD-inducible poly(ADP-ribose) polymerase-mediated antiviral response. *Proc Natl Acad Sci U S A* **114**(10), 2681-2686.

Kraus, W. L., and Hottiger, M. O. (2013). PARP-1 and gene regulation: Progress and puzzles. *Molecular aspects of medicine* **14**, 1109-1123.

Krig, S. R., and Rice, R. H. (2000). TCDD suppression of tissue transglutaminase stimulation by retinoids in malignant human keratinocytes. *Toxicol Sci* **56**(2), 357-64.

Lamas, B., Richard, M. L., Leducq, V., Pham, H. P., Michel, M. L., Da Costa, G., Bridonneau, C., Jegou, S., Hoffmann, T. W., Natividad, J. M.*, et al.* (2016).

CARD9 impacts colitis by altering gut microbiota metabolism of tryptophan into aryl hydrocarbon receptor ligands. *Nat Med* **22**(6), 598-605.

Lee, J. H., Wada, T., Febbraio, M., He, J., Matsubara, T., Lee, M. J., Gonzalez, F. J., and Xie, W. (2010). A novel role for the dioxin receptor in fatty acid metabolism and hepatic steatosis. *Gastroenterology* **139**(2), 653-63.

Li, T., Owsley, E., Matozel, M., Hsu, P., Novak, C. M., and Chiang, J. Y. (2010). Transgenic expression of cholesterol 7alpha-hydroxylase in the liver prevents high-fat diet-induced obesity and insulin resistance in mice. *Hepatology* **52**(2), 678-90.

Li, Y., Innocentin, S., Withers, D. R., Roberts, N. A., Gallagher, A. R., Grigorieva, E. F., Wilhelm, C., and Veldhoen, M. (2011). Exogenous stimuli maintain intraepithelial lymphocytes via aryl hydrocarbon receptor activation. *Cell* **147**(3), 629-40.

Linden, J., Lensu, S., Tuomisto, J., and Pohjanvirta, R. (2010). Dioxins, the aryl hydrocarbon receptor and the central regulation of energy balance. *Front Neuroendocrinol* **31**(4), 452-78.

Lo, R., Celius, T., Forgacs, A., Dere, E., MacPherson, L., Zacharewski, T., and Matthews, J. (2011). Identification of aryl hydrocarbon receptor binding targets in mouse hepatic tissue treated with 2,3,7,8-tetrachlorodibenzo-p-dioxin *Toxicol Appl Pharmacol* doi: 10.1016/j.taap.2011.08.016.

Lu, H., Cui, W., and Klaassen, C. D. (2011). Nrf2 protects against 2,3,7,8-tetrachlorodibenzo-p-dioxin (TCDD)-induced oxidative injury and steatohepatitis. *Toxicol Appl Pharmacol* **256**(2), 122-35.

Ma, Q., Baldwin, K. T., Renzelli, A. J., McDaniel, A., and Dong, L. (2001). TCDD-inducible poly(ADP-ribose) polymerase: a novel response to 2,3,7,8-tetrachlorodibenzo-p-dioxin. *Biochem Biophys Res Commun* **289**(2), 499-506.

MacPherson, L., Tamblyn, L., Rajendra, S., Bralha, F., McPherson, J. P., and Matthews, J. (2013). 2,3,7,8-tetrachlorodibenzo-p-dioxin poly(ADP-ribose) polymerase (TiPARP, ARTD14) is a mono-ADP-ribosyltransferase and repressor of aryl hydrocarbon receptor transactivation. *Nucleic Acids Res* **41**(3), 1604-21.

Marra, F., and Tacke, F. (2014). Roles for chemokines in liver disease. *Gastroenterology* **147**(3), 577-594 e1.

Matsubara, T., Tanaka, N., Krausz, K. W., Manna, S. K., Kang, D. W., Anderson, E. R., Luecke, H., Patterson, A. D., Shah, Y. M., and Gonzalez, F. J. (2012). Metabolomics identifies an inflammatory cascade involved in dioxin- and diet-induced steatohepatitis. *Cell metabolism* **16**(5), 634-44.

Matthews, J. (2017). AHR Toxicity and Signalling: Role of TIPARP and ADP-ribosylation. *Current Opinion in Toxicology* **2**, 50–57.

Mauvoisin, D., and Mounier, C. (2011). Hormonal and nutritional regulation of SCD1 gene expression. *Biochimie* **93**(1), 78-86.

Mimura, J., Ema, M., Sogawa, K., and Fujii-Kuriyama, Y. (1999). Identification of a novel mechanism of regulation of Ah (dioxin) receptor function. *Genes Dev* **13**(1), 20-5.

Monteleone, I., Rizzo, A., Sarra, M., Sica, G., Sileri, P., Biancone, L., MacDonald, T. T., Pallone, F., and Monteleone, G. (2011). Aryl hydrocarbon receptor-induced signals up-regulate IL-22 production and inhibit inflammation in the gastrointestinal tract. *Gastroenterology* **141**(1), 237-48, 248 e1.

Moura-Alves, P., Fae, K., Houthuys, E., Dorhoi, A., Kreuchwig, A., Furkert, J., Barison, N., Diehl, A., Munder, A., Constant, P.*, et al.* (2014). AhR sensing of bacterial pigments regulates antibacterial defence. *Nature* **512**, 387-392.

Nault, R., Fader, K. A., Ammendolia, D. A., Dornbos, P., Potter, D., Sharratt, B., Kumagai, K., Harkema, J. R., Lunt, S. Y., Matthews, J.*, et al.* (2016a). Dose-Dependent Metabolic Reprogramming and Differential Gene Expression in TCDD-Elicited Hepatic Fibrosis. *Toxicol Sci* **154**(2), 253-266.

Nault, R., Fader, K. A., Kirby, M. P., Ahmed, S., Matthews, J., Jones, A. D., Lunt, S. Y., and Zacharewski, T. R. (2016b). Pyruvate Kinase Isoform Switching and Hepatic Metabolic Reprogramming by the Environmental Contaminant 2,3,7,8-Tetrachlorodibenzo-p-Dioxin. *Toxicol Sci* **149**(2), 358-71.

Pohjanvirta, R., and Tuomisto, J. (1994). Short-term toxicity of 2,3,7,8-tetrachlorodibenzo-p-dioxin in laboratory animals: effects, mechanisms, and animal models. *Pharmacol Rev* **46**(4), 483-549.

Poland, A., and Knutson, J. C. (1982). 2,3,7,8-tetrachlorodibenzo-p-dioxin and related halogenated aromatic hydrocarbons: examination of the mechanism of toxicity. *Annu Rev Pharmacol Toxicol* **22**, 517-54.

Poland, A., Palen, D., and Glover, E. (1994). Analysis of the four alleles of the murine aryl hydrocarbon receptor. *Mol Pharmacol* **46**(5), 915-21.

Pullinger, C. R., Eng, C., Salen, G., Shefer, S., Batta, A. K., Erickson, S. K., Verhagen, A., Rivera, C. R., Mulvihill, S. J., Malloy, M. J.*, et al.* (2002). Human cholesterol 7alpha-hydroxylase (CYP7A1) deficiency has a hypercholesterolemic phenotype. *J Clin Invest* **110**(1), 109-17.

Quintana, F. J., Basso, A. S., Iglesias, A. H., Korn, T., Farez, M. F., Bettelli, E., Caccamo, M., Oukka, M., and Weiner, H. L. (2008). Control of T(reg) and T(H)17 cell differentiation by the aryl hydrocarbon receptor. *Nature* **453**(7191), 65-71.

Rouse, M., Singh, N. P., Nagarkatti, P. S., and Nagarkatti, M. (2013). Indoles mitigate the development of experimental autoimmune encephalomyelitis by induction of reciprocal differentiation of regulatory T cells and Th17 cells. *Br J Pharmacol* **169**(6), 1305-21.

Schmahl, J., Raymond, C. S., and Soriano, P. (2007). PDGF signaling specificity is mediated through multiple immediate early genes. *Nat Genet* **39**(1), 52-60.

Seefeld, M. D., Corbett, S. W., Keesey, R. E., and Peterson, R. E. (1984). Characterization of the wasting syndrome in rats treated with 2,3,7,8-tetrachlorodibenzo-p-dioxin. *Toxicol Appl Pharmacol* **73**(2), 311-22.

Son, D. S., and Rozman, K. K. (2002). 2,3,7,8-Tetrachlorodibenzo-p-dioxin (TCDD) induces plasminogen activator inhibitor-1 through an aryl hydrocarbon receptor-mediated pathway in mouse hepatoma cell lines. *Arch Toxicol* **76**(7), 404-13.

Stevens, E. A., Mezrich, J. D., and Bradfield, C. A. (2009). The aryl hydrocarbon receptor: a perspective on potential roles in the immune system. *Immunology* **127**(3), 299-311.

Stockinger, B., Di Meglio, P., Gialitakis, M., and Duarte, J. H. (2014). The aryl hydrocarbon receptor: multitasking in the immune system. *Annu Rev Immunol* **32**, 403-32.

Vogel, C. F., Chang, W. L., Kado, S., McCulloh, K., Vogel, H., Wu, D., Haarmann-Stemmann, T., Yang, G., Leung, P. S., Matsumura, F.*, et al.* (2016). Transgenic

Overexpression of Aryl Hydrocarbon Receptor Repressor (AhRR) and AhR-Mediated Induction of CYP1A1, Cytokines, and Acute Toxicity. *Environ Health Perspect* **124**(7), 1071-83.

Walisser, J. A., Glover, E., Pande, K., Liss, A. L., and Bradfield, C. A. (2005). Aryl hydrocarbon receptor-dependent liver development and hepatotoxicity are mediated by different cell types. *Proc Natl Acad Sci U S A*.

Whitlock, J. P., Jr. (1999). Induction of cytochrome P4501A1. *Annu Rev Pharmacol Toxicol* **39**, 103-25.

Xia, J., and Wishart, D. S. (2016). Using MetaboAnalyst 3.0 for Comprehensive Metabolomics Data Analysis. *Curr Protoc Bioinformatics* **55**, 14 10 1-14 10 91.

Yamada, T., Horimoto, H., Kameyama, T., Hayakawa, S., Yamato, H., Dazai, M., Takada, A., Kida, H., Bott, D., Zhou, A. C.*, et al.* (2016). Constitutive aryl hydrocarbon receptor signaling constrains type I interferon-mediated antiviral innate defense. *Nat Immunol* **17**(6), 687-94.

Zhang, L., Savas, U., Alexander, D. L., and Jefcoate, C. R. (1998). Characterization of the mouse Cyp1B1 gene. Identification of an enhancer region that directs aryl hydrocarbon receptor-mediated constitutive and induced expression. *J Biol Chem* **273**(9), 5174-83.

Figure Legends

Figure 1. Generation of the conditional *Tiparp*$^{fl/fl}$ mice. **(A)** Schematic diagram of *Tiparp* WT allele and the allele with successful recombination of the tm1 targeting construct (*Tiparp tm1a* allele) and corresponding Southern blot data. Exon numbers reflect known coding exons; white arrowheads represent FRT sites; grey arrowheads represent LoxP sites; LacZ represents lacZ reporter gene; N represents the neomycin (Neo) resistance cassette; S, SphI site; dashed lines indicate the fragment of DNA generated by SphI digestion that was detected with the radiolabeled probes (5` probe and Neo probe); letters indicate genotyping primers. **(B)** Southern blots show Tiparp allele fragments detected with the radiolabeled probes: ES clones D3 and G3 show correct homologous recombination of the targeting construct (12.3 kb fragment detected with 5` probe) without additional random integrations (only the 12.3 kb band detected with Neo probe). **(C)** Schematic diagram of *Tiparp tm1* alleles following excision of sequence by CRE or FLP recombinases. **(D)** PCR data from mouse tail biopsies. The *Tiparp* tm1a allele was converted to tm1b using CRE recombinase to remove the Neo cassette and exon 3 located between the LoxP sites. Primer pair D-E amplify a product spanning the excision sites to show that the floxed sequences were removed (420 bp). The *Tiparp* tm1a allele was converted to *tm1c* using FLP recombinase to remove the LacZ and Neo cassettes located between the FRT sites. Primer pair A-B amplify a product spanning the excision site to show that the sequence was flipped out (750 bp). The *Tiparp tm1c* allele was converted to *tm1d* using CRE recombinase to remove the floxed exon 3. Primer pair A-E amplify a product spanning the floxed region to show that the exon is removed (310 bp). Sample genotypes: + indicates the *Tiparp* WT allele; letters indicate the *Tiparp* tm1 corresponding allele (tm1a, tm1b, tm1c, tm1d).

Figure 2. Specificity of Cre^{Alb}-mediated excision of the *Tiparp*^{fl} allele. (**A**) Specificity of *Tiparp*^{fl} excision by Cre^{Alb} was determined by quantitative real-time PCR-based genotyping for excised and unexcised alleles of *Tiparp*^{fl} in genomic DNA isolated from various tissues and hepatocytes obtained from *Tiparp*$^{fl/fl}$ and *Tiparp*$^{fl/fl}$*Cre*^{Alb} mice. * $p < 0.05$ compared with tissue matched *Tiparp*$^{fl/fl}$ mice. (**B**) *Tiparp*^{fl} excision by Cre^{CMV} was determined from genomic DNA isolated from livers of *Tiparp*$^{+/+}$ and *Tiparp*$^{Ex3-/-}$ mice. Hep, hepatocytes; WAT, white adipose tissue. (**C**) Increased AHR regulated Cyp1a1, Cyp1a2, Cyp1b1 and Tiparp mRNA levels in expression in hepatocytes isolated from *Tiparp*$^{fl/fl}$ and *Tiparp*$^{fl/fl}$*Cre*^{Alb} mice treated with 10 nM dioxin for 6 h. RNA and qPCR were performed as described in the materials and methods section. * $p < 0.05$ compared with genotyped match control treated, # $p < 0.05$ compared with dioxin-treated *Tiparp*$^{fl/fl}$, $n = 3$.

Figure 3. AHR regulated transcript levels in liver and lung tissue isolate from control and dioxin-treated *Tiparp*$^{Ex3-/-}$, *Tiparp*$^{fl/fl}$*Cre*^{Alb} and their respective WT mice. Mice were treated with a single injection of 100 μg/kg dioxin in DMSO, or DMSO vehicle alone, and euthanized 6 h later. RNA and qPCR were performed as described in the materials and methods section. * $p < 0.05$ compared with genotype matched control-treated; # $p < 0.05$ compared with dioxin-treated *Tiparp*$^{+/+}$ (**A-C**) or *Tiparp*$^{fl/fl}$ (**D-F**), n = 4.

Figure 4. Loss of TIPARP increases dioxin-induced hepatotoxicity and lethal wasting syndrome in male mice. (**A**) Kaplan-Meier survival curves for male *Tiparp*$^{+/+}$ and *Tiparp*$^{Ex3-/-}$ mice treated with a single 10 or 100 μg/kg i.p. injection of dioxin and monitored for 30 days. (**B**) Body weight, (**C**) food intake, (**D**) serum alanine aminotransferase (ALT) activity, (**E**) liver, (**F**) thymus and (**G**) WAT weight expressed as percentage of total body weight, and (**H**) hepatic glycogen levels were measured from *Tiparp*$^{+/+}$ and *Tiparp*$^{Ex3-/-}$ mice treated with 10 μg/kg dioxin. Data shown are the mean ± SEM. n = 4-5. For (**B-G**) $^{*}P < 0.05$, two-way ANOVA followed by Tukey's post-hoc test compared with genotype-matched control treated mice. For (**H**) $^{*}P < 0.05$, Student's t-test.

Figure 5. Hepatocyte-specific loss of TIPARP increases dioxin-induced hepatotoxicity and lethal wasting syndrome in male mice. (**A**) Kaplan-Meier survival curves for male *Tiparp*$^{fl/fl}$ and *Tiparp*$^{fl/fl}$*Cre*^{Alb} mice treated with a single 10 or 100 μg/kg i.p. injection of dioxin and monitored for 30 days. (**B**) Body weight, (**C**) food intake, (**D**) serum alanine aminotransferase (ALT) activity, (**E**) liver, (**F**) thymus and (**G**) WAT weight expressed as percentage of total body weight, and (**H**) hepatic glycogen levels were measured from *Tiparp*$^{fl/fl}$ and *Tiparp*$^{fl/fl}$*Cre*^{Alb} mice treated with 10 μg/kg dioxin. Data shown are the mean ± SEM. n = 4-5. For (**B-G**) $^{*}P < 0.05$, two-way ANOVA followed by Tukey's post-hoc test compared with genotype-matched control treated mice. For (**H**) $^{*}P < 0.05$, Student's t-test.

Figure 6. Increased liver inflammation and cytokine levels in dioxin-treated *Tiparp*$^{fl/fl}$*Cre*^{Alb} compared with *Tiparp*$^{fl/fl}$ mice. (**A**) Representative H&E staining of livers from *Tiparp*$^{fl/fl}$ and *Tiparp*$^{fl/fl}$*Cre*^{Alb} mice (n=4). Control animals were injected with CO and were euthanized on day 9. The asterisks (*****) indicate focal inflammatory infiltration, and the arrowheads indicate microvesicular steatosis. All images are to the same scale. Hepatic (**B**) *Il6*, (**C**) *Serpine 1*, (**D**) *Cxcl2*, and (**E**) *F4/80* mRNA levels were determined as described in the methods. Data represent the mean ± SEM (n=4). $^{*}P<0.05$ two-way ANOVA compared with genotyped-matched control treated mice. $^{\#}P<0.05$ two-way ANOVA compared with dioxin-treated *Tiparp*$^{fl/fl}$ mice.

Figure 7. Dioxin-induced steatosis is increased in *Tiparp*$^{fl/fl}$*Cre*^{Alb} mice. (**A**) Livers from male *Tiparp*$^{fl/fl}$ and *Tiparp*$^{fl/fl}$*Cre*^{Alb} mice given a single i.p. injection of CO or 10 μg/kg dioxin and euthanized after 9 days (*n*=5). (**B**) Oil-Red-O and hematoxylin stained liver sections from *Tiparp*$^{fl/fl}$ and *Tiparp*$^{fl/fl}$*Cre*^{Alb} mice. All images are to the same scale. Hepatic mRNA levels of *Cd36* (**C**), *Scd1* (**D**), *Srebp1* (**E**), *Ppara* (**F**) and *Cyp7a1* (**G**) were determined as described in the methods. Data represent the mean ± SEM (*n*=4). For all data, $P < 0.05$ was determined by Two-way ANOVA followed by Tukey's post-hoc test comparison. Significantly different compared with genotype-matched *DMSO- or $^{\#}$dioxin-treated *Tiparp*$^{fl/fl}$ mice.

Figure 8. Hepatocyte-specific loss of TIPARP increases dioxin-dependent regulation of hepatic AHR target gene expression. Hepatic mRNA levels of *Cyp1a1* **(A)**, *Cyp1a2* **(B)**, *Cyp1b1* **(C)**, *Tiparp* **(D)**, *Ahrr* **(E)** *Nqo1* **(F)** *Nfe2l2* **(G)** *Serpine 1* **(H)** were determined after 3 days of exposure to corn oil or 10 μg/kg dioxin as described in experimental procedures (*n*=4). Recruitment of AHR to *Cyp1a1* **(I)** and *Cyp1b1* **(J)**. Data represent the mean ± SEM. Representative AHR **(K)**, and β-actin protein levels were detected by Western blotting after 3 days of treatment. AHR proteins levels were normalized to β-actin levels, *n*=4) **(L)**. For all data, $P < 0.05$ was determined by Two-way ANOVA followed by Tukey's post-hoc test comparison. Significantly different compared with genotype-matched *DMSO- or $^{\#}$dioxin-treated *Tiparp*$^{fl/fl}$ mice.

Figure 9. Dioxin-induced hepatic metabolomic disruption. **(A)** Principal Component Analysis (PCA) of hepatic metabolomic analysis after 3 day treatment of *Tiparp*$^{fl/fl}$ (*fl/fl*) and *Tiparp*$^{fl/fl}$*Cre*^{Alb} with corn oil (CO) or 10 μg/kg dioxin. **(B)** Venn diagram of the overlapping metabolites that were significantly altered between dioxin treated *Tiparp*$^{fl/fl}$ and *Tiparp*$^{fl/fl}$*Cre*^{Alb}. Metabolic pathway enrichment analysis of altered hepatic metabolites ($P < 0.05$) in dioxin-treated *Tiparp*$^{fl/fl}$*Cre*^{Alb} **(C)** and *Tiparp*$^{fl/fl}$ mice **(D)**. Hepatic levels of gamma-glutamyl-epsilon lysine **(E)**, N-acetylputrescine **(F)**, putrescine **(G)**, nicotinamde ribonucleoside **(H)**, nicotinamide **(I)** and NAD^{+} **(J)**. Data represent the mean ± SEM (*n*=6-8).

Table 1. A summary of the numbers of biochemicals that achieved statistical significance ($p \leq 0.05$) among the different comparisons.

	Statistical Comparisons			
ANOVA Contrasts	$\frac{Tiparp^{fl/fl}\ TCDD}{Tiparp^{fl/fl}\ CO}$	$\frac{Tiparp^{fl/fl}Cre^{Alb}\ TCDD}{Tiparp^{fl/fl}Cre^{Alb}\ CO}$	$\frac{Tiparp^{fl/fl}Cre^{Alb}\ CO}{Tiparp^{fl/fl}\ CO}$	$\frac{Tiparp^{fl/fl}Cre^{Alb}\ TCDD}{Tiparp^{fl/fl}\ TCDD}$
Total Biochemicals $p<0.05$	124	213	7	129
Biochemicals (up | down)	75 | 49	163 | 50	4 | 3	111 | 18

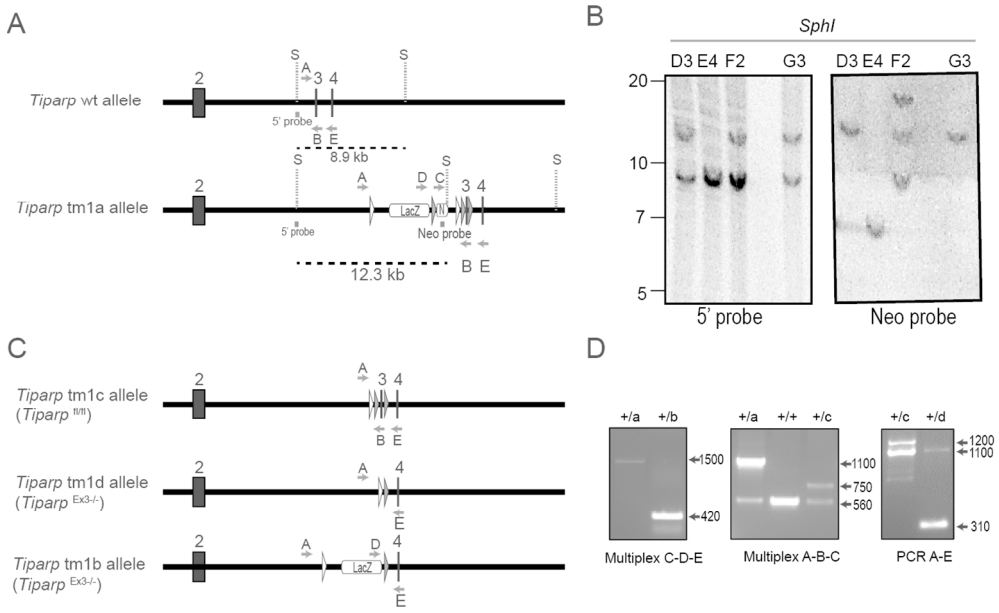

Figure 1. Generation of the conditional Tiparpfl/fl mice. (A) Schematic diagram of Tiparp WT allele and the allele with successful recombination of the tm1 targeting construct (Tiparp tm1a allele) and corresponding Southern blot data. Exon numbers reflect known coding exons; white arrowheads represent FRT sites; grey arrowheads represent LoxP sites; LacZ represents lacZ reporter gene; N represents the neomycin (Neo) resistance cassette; S, SphI site; dashed lines indicate the fragment of DNA generated by SphI digestion that was detected with the radiolabeled probes (5` probe and Neo probe); letters indicate genotyping primers. (B) Southern blots show Tiparp allele fragments detected with the radiolabeled probes: ES clones D3 and G3 show correct homologous recombination of the targeting construct (12.3 kb fragment detected with 5` probe) without additional random integrations (only the 12.3 kb band detected with Neo probe). (C) Schematic diagram of Tiparp tm1 alleles following excision of sequence by CRE or FLP recombinases. (D) PCR data from mouse tail biopsies. The Tiparp tm1a allele was converted to tm1b using CRE recombinase to remove the Neo cassette and exon 3 located between the LoxP sites. Primer pair D-E amplify a product spanning the excision sites to show that the floxed sequences were removed (420 bp). The Tiparp tm1a allele was converted to tm1c using FLP recombinase to remove the LacZ and Neo cassettes located between the FRT sites. Primer pair A-B amplify a product spanning the excision site to show that the sequence was flipped out (750 bp). The Tiparp tm1c allele was converted to tm1d using CRE recombinase to remove the floxed exon 3. Primer pair A-E amplify a product spanning the floxed region to show that the exon is removed (310 bp). Sample genotypes: + indicates the Tiparp WT allele; letters indicate the Tiparp tm1 corresponding allele (tm1a, tm1b, tm1c, tm1d).

125x77mm (300 x 300 DPI)

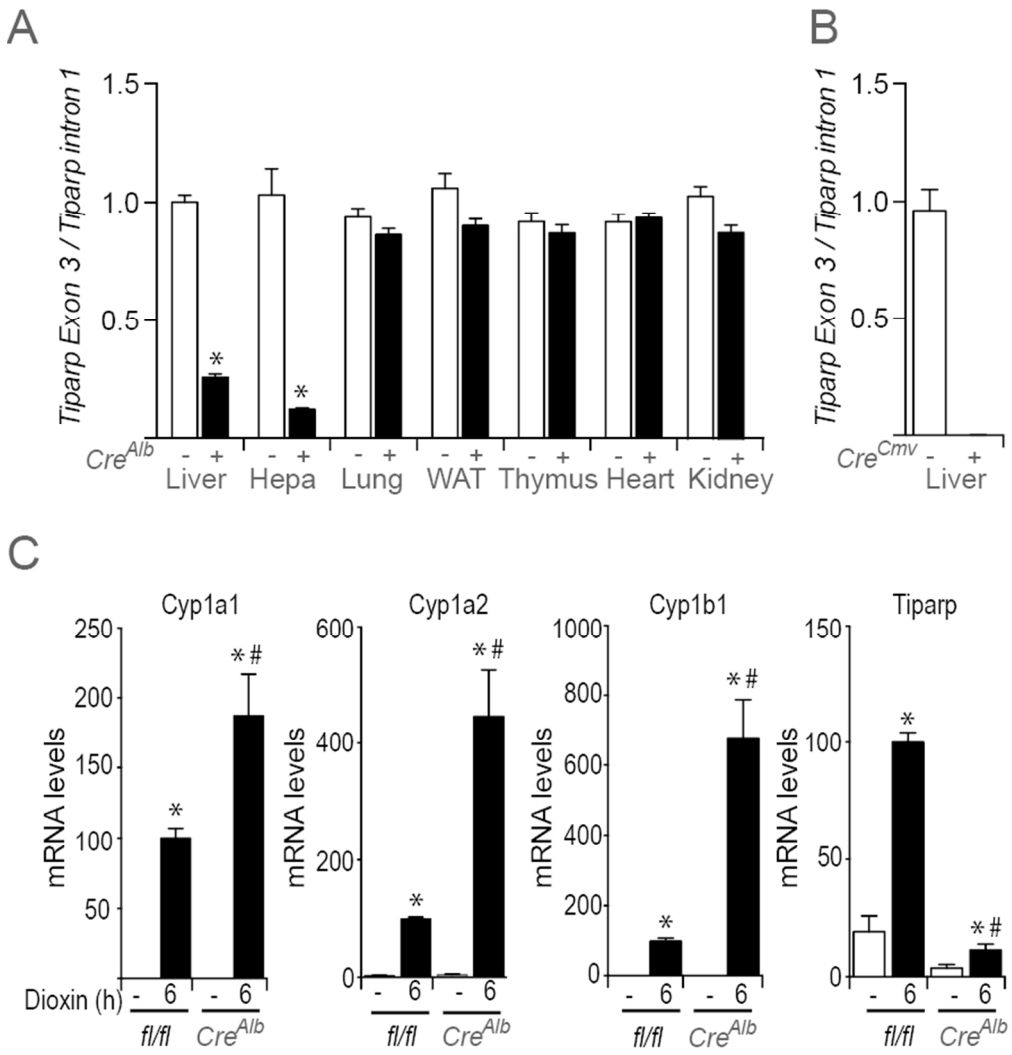

Figure 2. Specificity of CreAlb-mediated excision of the Tiparpfl allele. (A) Specificity of Tiparpfl excision by CreAlb was determined by quantitative real-time PCR-based genotyping for excised and unexcised alleles of Tiparpfl in genomic DNA isolated from various tissues and hepatocytes obtained from Tiparpfl/fl and Tiparpfl/flCreAlb mice. * $p < 0.05$ compared with tissue matched Tiparpfl/fl mice. (B) Tiparpfl excision by CreCMV was determined from genomic DNA isolated from livers of Tiparp+/+ and TiparpEx3-/- mice. Hep, hepatocytes; WAT, white adipose tissue. (C) Increased AHR regulated Cyp1a1, Cyp1a2, Cyp1b1 and Tiparp mRNA levels in expression in hepatocytes isolated from Tiparpfl/fl and Tiparpfl/flCreAlb mice treated with 10 nM dioxin for 6 h. RNA and qPCR were performed as described in the materials and methods section. * $p < 0.05$ compared with genotyped match control treated, # $p < 0.05$ compared with dioxin-treated Tiparpfl/fl, n = 3.

75x78mm (300 x 300 DPI)

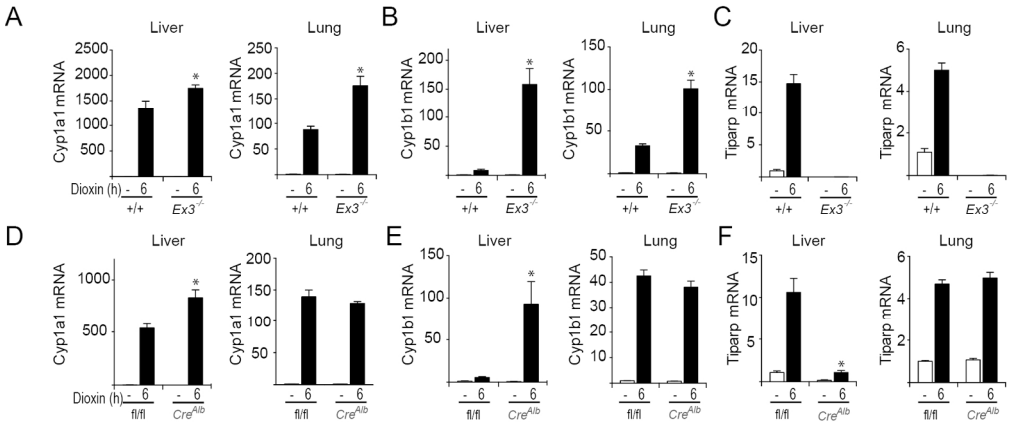

Figure 3. AHR regulated transcript levels in liver and lung tissue isolate from control and dioxin-treated TiparpEx3-/-, Tiparpfl/flCreAlb and their respective WT mice. Mice were treated with a single injection of 100 µg/kg dioxin in DMSO, or DMSO vehicle alone, and euthanized 6 h later. RNA and qPCR were performed as described in the materials and methods section. * $p < 0.05$ compared with genotype matched control-treated; # $p < 0.05$ compared with dioxin-treated Tiparp+/+ (A-C) or Tiparpfl/fl (D-F), n = 4.

160x67mm (300 x 300 DPI)

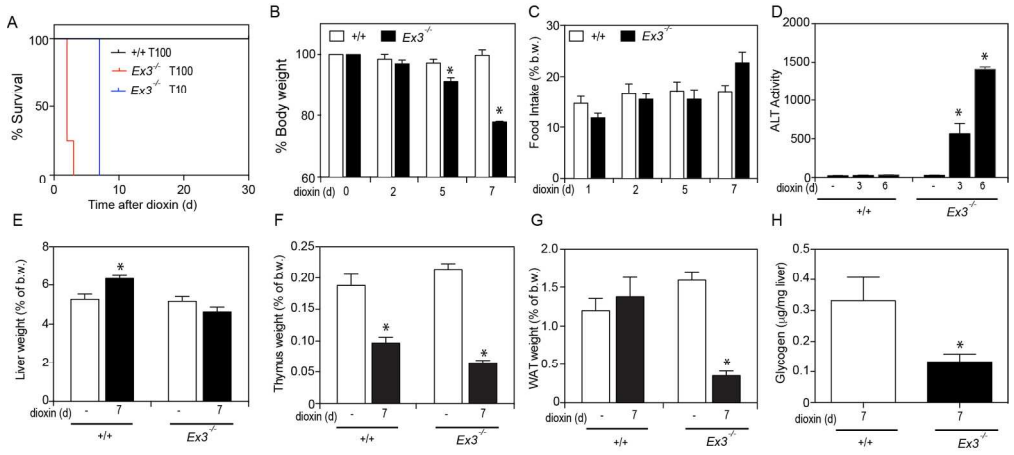

Figure 4. Loss of TIPARP increases dioxin-induced hepatotoxicity and lethal wasting syndrome in male mice. (A) Kaplan-Meier survival curves for male Tiparp+/+ and TiparpEx3-/- mice treated with a single 10 or 100 µg/kg i.p. injection of dioxin and monitored for 30 days. (B) Body weight, (C) food intake, (D) serum alanine aminotransferase (ALT) activity, (E) liver, (F) thymus and (G) WAT weight expressed as percentage of total body weight, and (H) hepatic glycogen levels were measured from Tiparp+/+ and TiparpEx3-/- mice treated with 10 µg/kg dioxin. Data shown are the mean ± SEM. n = 4-5. For (B-G) *P < 0.05, two-way ANOVA followed by Tukey's post-hoc test compared with genotype-matched control treated mice. For (H) *P < 0.05, Student's t-test.

172x77mm (300 x 300 DPI)

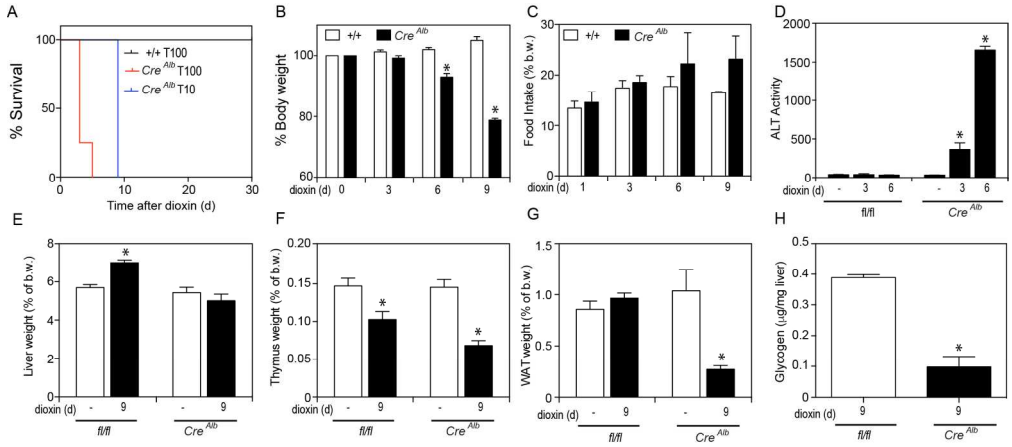

Figure 5. Hepatocyte-specific loss of TIPARP increases dioxin-induced hepatotoxicity and lethal wasting syndrome in male mice. (A) Kaplan-Meier survival curves for male Tiparpfl/fl and Tiparpfl/flCreAlb mice treated with a single 10 or 100 µg/kg i.p. injection of dioxin and monitored for 30 days. (B) Body weight, (C) food intake, (D) serum alanine aminotransferase (ALT) activity, (E) liver, (F) thymus and (G) WAT weight expressed as percentage of total body weight, and (H) hepatic glycogen levels were measured from Tiparpfl/fl and Tiparpfl/flCreAlb mice treated with 10 µg/kg dioxin. Data shown are the mean ± SEM. n = 4-5. For (B-G) *P < 0.05, two-way ANOVA followed by Tukey's post-hoc test compared with genotype-matched control treated mice. For (H) *P < 0.05, Student's t-test.

173x77mm (300 x 300 DPI)

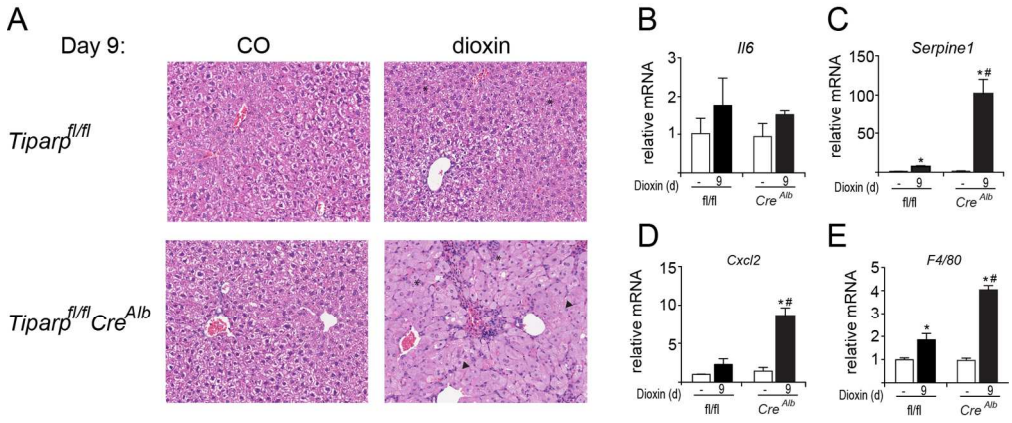

Figure 6. Increased liver inflammation and cytokine levels in dioxin-treated Tiparpfl/flCreAlb compared with Tiparpfl/fl mice. (A) Representative H&E staining of livers from Tiparpfl/fl and Tiparpfl/flCreAlb mice (n=4). Control animals were injected with CO and were euthanized on day 9. The asterisks (*) indicate focal inflammatory infiltration, and the arrowheads indicate microvesicular steatosis. All images are to the same scale. Hepatic (B) Il6, (C) Serpine 1, (D) Cxcl2, and (E) F4/80 mRNA levels were determined as described in the methods. Data represent the mean ± SEM (n=4). *P<0.05 two-way ANOVA compared with genotyped-matched control treated mice. #P<0.05 two-way ANOVA compared with dioxin-treated Tiparpfl/fl mice.

156x65mm (300 x 300 DPI)

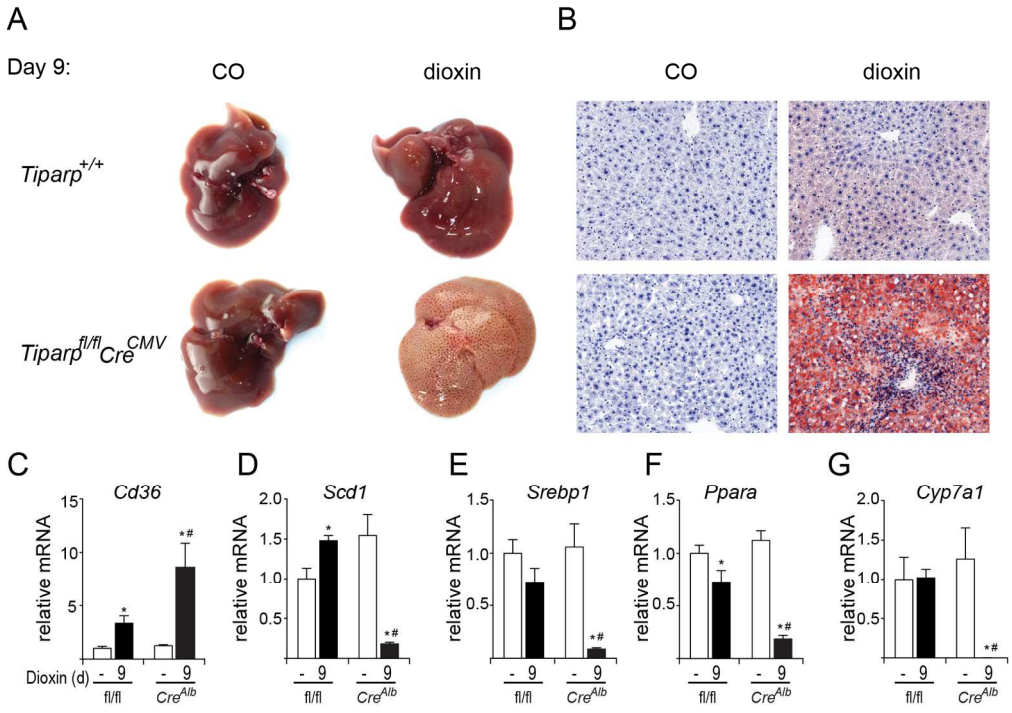

Figure 7. Dioxin-induced steatosis is increased in Tiparpfl/flCreAlb mice. (A) Livers from male Tiparpfl/fl and Tiparpfl/flCreAlb mice given a single i.p. injection of CO or 10 µg/kg dioxin and euthanized after 9 days (n=5). (B) Oil-Red-O and hematoxylin stained liver sections from Tiparpfl/fl and Tiparpfl/flCreAlb mice. All images are to the same scale. Hepatic mRNA levels of Cd36 (C), Scd1 (D), Srebp1 (E), Ppara (F) and Cyp7a1 (G) were determined as described in the methods. Data represent the mean ± SEM (n=4). For all data, $P < 0.05$ was determined by Two-way ANOVA followed by Tukey's post-hoc test comparison. Significantly different compared with genotype-matched *DMSO- or #dioxin-treated Tiparpfl/fl mice.

159x123mm (300 x 300 DPI)

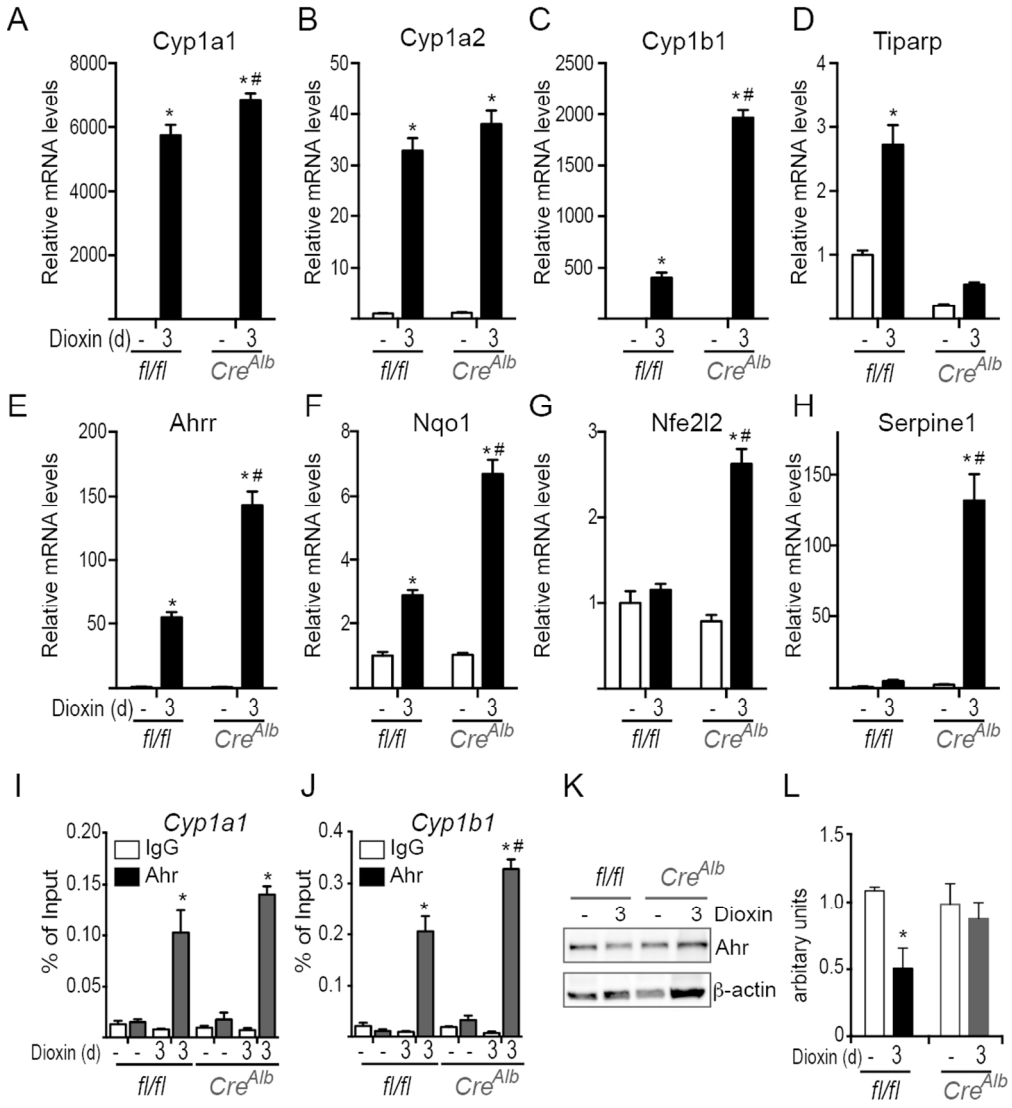

Figure 8. Hepatocyte-specific loss of TIPARP increases dioxin-dependent regulation of hepatic AHR target gene expression. Hepatic mRNA levels of Cyp1a1 (A), Cyp1a2 (B), Cyp1b1 (C), Tiparp (D), Ahrr (E) Nqo1 (F) Nfe2l2 (G) Serpine 1 (H) were determined after 3 days of exposure to corn oil or 10 μg/kg dioxin as described in experimental procedures (n=4). Recruitment of AHR to Cyp1a1 (I) and Cyp1b1 (J). Data represent the mean ± SEM. Representative AHR (K), and β-actin protein levels were detected by Western blotting after 3 days of treatment. AHR proteins levels were normalized to β-actin levels, n=4) (L). For all data, $P < 0.05$ was determined by Two-way ANOVA followed by Tukey's post-hoc test comparison. Significantly different compared with genotype-matched *DMSO- or #dioxin-treated Tiparpfl/fl mice.

99x109mm (300 x 300 DPI)

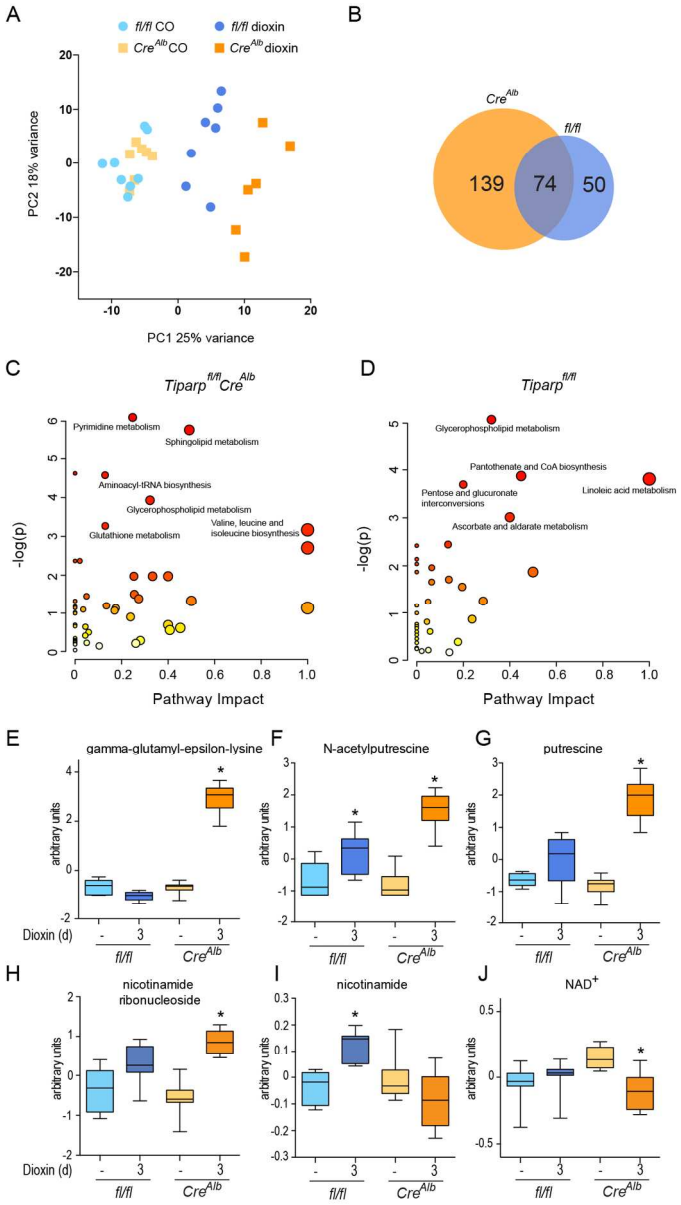

Figure 9. Dioxin-induced hepatic metabolomic disruption. (A) Principal Component Analysis (PCA) of hepatic metabolomic analysis after 3 day treatment of Tiparpfl/fl (fl/fl) and Tiparpfl/flCreAlb with corn oil (CO) or 10 µg/kg dioxin. (B) Venn diagram of the overlapping metabolites that were significantly altered between dioxin treated Tiparpfl/fl and Tiparpfl/flCreAlb. Metabolic pathway enrichment analysis of altered hepatic metabolites ($P < 0.05$) in dioxin-treated Tiparpfl/flCreAlb (C) and Tiparpfl/fl mice (D). Hepatic levels of gamma-glutamyl-epsilon lysine (E), N-acetylputrescine (F), putrescine (G), nicotinamde ribonucleoside (H), nicotinamide (I) and NAD+ (J). Data represent the mean ± SEM (n=6-8).

109x196mm (300 x 300 DPI)